



# Enrichment of lignin reveals consistent anaerobic degradation and persistent vegetation signatures in the organic matter of diverse lowland tropical peatland profiles

Mike Vreeken<sup>1</sup>, Megan N. Jenkins<sup>1</sup>, Siwei Mai<sup>1</sup>, Rebecca H. Peel<sup>1</sup>, Yiming Zhang<sup>1</sup>, Toby A. Halamka<sup>1</sup>,  
5 Amelia Oakeshott<sup>2</sup>, Simon M. K. Cheung<sup>2</sup>, Panteleimon Prokopiou<sup>1</sup>, Sam Rangdale<sup>1</sup>, Jerome Blewett<sup>1</sup>,  
D. Paola Alarcon Prado<sup>2</sup>, Juan C. Benavides<sup>3</sup>, Frank Kansime<sup>4</sup>, Ellen Kayendeke<sup>4</sup>, Carol Kagaba  
Kairumba<sup>5</sup>, B. David A. Naafs<sup>1</sup>, Casey Bryce<sup>2</sup>, Angela V. Gallego-Sala<sup>6</sup>, Richard D. Pancost<sup>1</sup>

<sup>1</sup>Organic Geochemistry Unit, Schools of Chemistry and Earth Sciences, University of Bristol, Bristol, BS8 1TS, United  
10 Kingdom

<sup>2</sup>School of Earth Sciences, University of Bristol, Bristol, BS8 1RJ, United Kingdom

<sup>3</sup>Department of Ecology and Territory, Pontificia Universidad Javeriana, Bogota, 110231, Colombia

<sup>4</sup>Department of Environmental Management, Makerere University, Kampala, P.O. Box 7298, Uganda

<sup>5</sup>Wetlands Management Department, Ministry of Water and Environment, Kampala, P.O. Box 20026, Uganda

15 <sup>6</sup>Department of Geography, University of Exeter, Exeter, EX4 4QE, United Kingdom

*Correspondence to:* Mike Vreeken ([mike.vreeken@bristol.ac.uk](mailto:mike.vreeken@bristol.ac.uk))

**Abstract.** Tropical peatlands store a significant amount of carbon but are also one of the most vulnerable carbon stocks due  
to anthropogenic pressures and climate change. The stability and accumulation of the organic carbon stored in tropical peat  
20 systems, and its sensitivity to changing temperature and/or hydrology, is intrinsically linked to the organic matter (OM)  
character. However, we currently lack a detailed understanding of the OM characteristics in tropical peatlands, hindering the  
accurate prediction of tropical peatland stability in the 21st century.

In this study, we characterise the macromolecular composition of peatland vegetation, leaf litter, and across peat depth  
25 profiles using a range of tropical ( $n = 7$ ) and some temperate ( $n = 2$ ) peatland ecosystems that serve as comparison. This  
characterisation is achieved primarily via Pyrolysis Gas Chromatography Mass Spectrometry (Py-GC-MS), complemented  
by Fourier-Transform Infrared Spectroscopy (FTIR). We find that silicate mineral interference in hydrologically active sites  
makes FTIR challenging to apply in these tropical systems. Our results also demonstrate that all sites exhibit distinct pools of  
putatively labile and recalcitrant (plant) OM, with both shared and distinct downcore degradation features. Most sites exhibit  
30 a downcore relative enrichment in aromatic pyrolysates, such as from lignin, vs polysaccharide pyrolysates. This relative  
enrichment follows a logarithmic decline, especially in the anoxic horizons. Regardless of the decomposition of the peat,  
however, a pyrolytic fingerprint of the original vegetation persists. This unique fingerprint is likely a driver behind the  
microbial community's speciality to degrade the OM in its specific peatland, an effect known as the home advantage theory.  
The predictable preferential loss of polysaccharides at depth and consistent aromaticity of the leaf litter in the tropical sites



35 can aid peatland accumulation modelling and enable more accurate predictions of peatland dynamics under future climate change.

## 1 Introduction

Peatlands cover only 3% of Earth's surface but play a key role in global carbon cycle. Pristine peatlands act as a global sink of around 0.14 Gt of carbon a year (Gallego-Sala et al., 2018) and at the same time are a main natural source of the potent  
40 greenhouse gas methane (Sjögersten et al., 2018). The global carbon stock of peatlands is estimated to be in the range of 500–700 Pg C (Yu et al., 2010; Nichols and Petecet, 2019), which is roughly equal to the amount of carbon in the preindustrial atmosphere (Gallego-Sala et al., 2018). Most of this carbon is stored in temperate/boreal peatlands, but historically, lowland tropical peatland carbon stocks have been underestimated. Currently, tropical peatlands are estimated to store approximately 105 Gt of carbon (Page et al., 2022), but on a smaller land area than temperate and boreal peatlands,  
45 making them more carbon dense and more sensitive to change (Cole et al., 2022).

However, the peatland carbon sink is expected to shift to a source under anthropogenic climate change (Loisel et al., 2020) and in some scenarios is a source already (Leifeld et al., 2019). Tropical wetlands, which include peatlands, have already been invoked as a main driver of the observed increase in atmospheric methane emissions over the past decade (Michel et al., 2024; Peng et al., 2022), albeit contested (Xiong et al., 2025), attesting to the need for a more fundamental understanding  
50 of tropical peatland carbon dynamics in response to climate change.

There is a wide range of processes that threaten the stability of peatlands, including temperature change, atmospheric pollution, sea level change, fire frequency, permafrost melting, changes in precipitation and moisture balance, and land use  
55 change (Page and Baird, 2016; Loisel et al., 2020). Alternatively, restoration of peatlands holds the potential to enhance the sink capabilities and is a major part of climate mitigation strategies (Leifeld and Menichetti, 2018). Because of the wide range of processes involved, the sensitivity of peatlands to future environmental changes is hard to predict. For example, in the absence of other factors, global warming is predicted to transform peatlands from a carbon sink into a source on a global scale after 2100 (Gallego-Sala et al., 2018; Rosset et al., 2022). Land use change in this century by drainage of tropical  
60 peatlands and subsequent OM (organic matter) degradation will accelerate this process and emit large quantities of carbon to the atmosphere (Girkin et al., 2022). However, many uncertainties remain. Constraining the biogeochemistry of these systems and the chemical composition of tropical peat is therefore key to understanding how ongoing and future disturbances will impact peatland carbon stocks.

65 An important factor in the carbon balance of peatlands is the chemical composition of the OM, which imparts a significant control on OM reactivity (Wright et al., 2011). Recent work highlighted the important role of carbohydrate vs aromatic peat



composition, with carbohydrate-rich peat generally being more reactive and associated with lower accumulation rates compared to aromatic peat (Normand et al., 2021; Könönen et al., 2016). Because of the association of carbohydrates with plant cellulose and hemicellulose and aromatic components with lignin, differences in peat chemical composition predominantly arise from the difference in dominant peat-forming vegetation, and this difference is manifested on a global scale (Verbeke et al., 2022). For example, lowland tropical peats are often characterised by much more lignin-rich OM compared to temperate/boreal peatlands because of woodier vegetation in the tropics (Page et al., 2022; Chimner and Ewel, 2005). In addition, OM in lowland tropical peatlands consists of lignin-rich roots and stems which grow in the peat soil, nestled into the anaerobic horizon (Hoyos-Santillan et al., 2015; Chimner and Ewel, 2005). Additionally, lowland tropical peatlands are associated with higher mean annual air temperature (20–30°C) and subsequently have higher rates of OM degradation compared to temperate and especially boreal peats (Page et al., 2022), which further enriches the relative abundance of OM with recalcitrant (i.e. aromatic) components. Therefore, on a global scale, aromatic compounds are enriched in high temperature, tropical compared to temperate/boreal peatlands (Verbeke et al., 2022; Normand et al., 2021).

However, there remain profound gaps in our overall understanding of peatland OM composition and variability, especially for the tropics. These include: *i*) a lack of investigations across a range of peat-forming vegetation and a systematic survey of different peatland types (Dehaen et al., 2025; Hoyos-Santillan et al., 2015); *ii*) relatively few deep downcore investigations that allow characterisation of deep (>50 cm) peat or understanding of how OM composition varies with depth and level of degradation (Schellekens et al., 2012); and *iii*) most studies rely on Fourier-Transform Infrared Spectroscopy (FTIR) that can reconstruct carbohydrate vs aromatic contributions, but lacks the nuance of other analytical methods (Hodgkins et al., 2018). Consequently, predictions for future impacts on peatland carbon stocks are incomplete and biased towards (temperate/boreal) surface/shallow peat, and our OM model for peatlands is lacking the detailed and granular understanding required to accurately predict its response to anthropogenic climate change during the 21<sup>st</sup> century (Verbeke et al., 2022; Dehaen et al., 2025).

Therefore, we have characterised the (non-extractable) bulk OM of peatland vegetation, leaf litter, and peat depth profiles from a range of lowland tropical (n = 7) and some temperate (n = 2) peatland ecosystems. The lowland tropical sites include palm, hardwood forest, sawgrass and papyrus swamps, and the two temperate sites include an ombrotrophic bog and a minerotrophic fen that serve as a comparison. We characterise all plant and peat OM primarily via Pyrolysis Gas Chromatography Mass Spectrometry (py-GC-MS) (Boon et al., 1986), complemented by FTIR (Given et al., 1984). We first identify major differences in the OM composition of peat-forming vegetation and use these data to identify plant biopolymer transformations throughout the peat profile. From these, we explore the factors that likely drive the recalcitrance of the OM in our sites. Lastly, we extract major trends in our globally representative lowland tropical peat survey and discuss the implications for our understanding of peatland accumulation and stability.



## 100 2 Methods

### 2.1 Site descriptions

#### 2.1.1 Everglades, USA

The Everglades (USWCA1; 26°30'18.0"N 80°15'52.0"W) is a 6000 km<sup>2</sup>, sub-tropical wetland in Florida, USA, which features patches of peat accumulation as old as ~ 4000 years (Wright and Comas, 2016). The mean annual temperature is ~  
105 23 °C (Abteu et al., 2011), and mean annual precipitation is ~ 1500 mm, with 75% of this falling during the wet summer season (Abiy et al., 2019). Sampling was conducted in early May 2019, at the start of the wet season. A 2 m core was collected from the Loxahatchee National Wildlife Refuge's Water Conservation Area 1 (WCA1). In this part of the Everglades, the peat visibly consists of *Nymphaea odorata* water lily remains, although *Cladium mariscus* stands exist nearby. At present, WCA1 is affected by elevated nutrient levels due to agricultural runoff, but this is a relatively recent  
110 phenomena and hence does not reflect nutrient levels during most of the peat deposition (Wang et al., 2009; Wright et al., 2008). At the coring location, the water table is likely continuously above the peat surface (Blewett et al., 2020).

#### 2.1.2 Amacayacu, Colombia

Parque Nacional Natural Amacayacu (PNN Amacayacu; 267,241 ha) is a national natural park in the Colombian Amazon (Amazonas Department, southern Colombia), extending from the Cotuhe River in the north to the Colombian bank of the  
115 Amazon River in the south, between the mouths of the Amacayacu River and the Matamata creek from which two peatlands are used in this study. The park has a tropical rainforest climate under a unimodal rainfall regime with a mean annual precipitation of ~ 3300 mm. The lowest monthly rainfall occurs in July/August and wet season peaking in March-April. The average temperature is ~ 26 °C with little seasonal variation and the humidity exceeds 90% (IDEAM Aeropuerto Vasquez Cobo, Leticia).

120

The Cananguchal site (CAC; 3°48'25.4"S 70°13'40.3"W) is a palm swamp peatland (locally known as cananguchal; equivalent to aguajal in Peru and buritizal in Brazil) located approximately 3 km from the Amazon River near Mocagua, in the southern sector of PNN Amacayacu. Despite its proximity to the Amazon River, it is predominantly rain-fed but with potential lateral runoff inputs from surrounding terra firme. The swamp is dominated by the *Mauritia flexuosa* L.f.  
125 (Arecaceae) palm with minor vegetation members including stunted *Ceiba pentandra* (L.) Gaertn and members of the Melastomataceae family. The peat depth at the centre averages around 1.5m with peat initiation ~ 600 cal yr BP (Table S5). Sampling was conducted in August 2023 using a Russian corer until basement at 1.53 m.

Pantano (CAP; 3°48'50.5"S 70°16'03.5"W) is an herbaceous peat swamp on the banks of the Amazon River, which connects  
130 to the swamp during wet season and features many underground streams that feed and drain the swamp continuously. The primary vegetation is *Montrichardia arborescens* (L.) Schott (Araceae) at the centre of the peatland, while stunted trees such



as *Triplaris americana* (Tangarana), *Ficus sp.* (Matapalo) and *Pachira sp.* (Punga) become more dominant together with *Cyperus articulatus* (Piri Piri) at the edges (Table S2). Due to atypically wet conditions during our sampling campaign that took place in the peak dry season (August 2023), cores were collected at the edge of the peatland. A monolith and a deeper  
135 Russian core were recovered, both exhibiting a gradual transition from primarily peat material at 0.45 m to a clay/organic mixture at 0.76 m.

### 2.1.3 Inírida Hardwood Swamp, Colombia

The hardwood swamp close to Inírida (CIH; 3°45'02.6"N 67°49'45.7"W) features an uncharacterized community of tropical rainforest species with a dominance of hardwood trees. Mean annual precipitation is ~ 3100 mm, with a dry season in  
140 January/February and wet season in June/July, and a mean temperature of ~ 26 °C (IDEAM Puerto Inírida). The swamp features a characteristic basement of white sand, which makes it a representative of the white-sand forest class of Amazonian peatlands (Winton et al., 2025; Draper et al., 2018). A 0.75 m long core was taken using a Russian corer in August 2023.

### 2.1.4 San San Pond Sak, Panama

San San Pond Sak (SSPS) is a wetland area covering 164 km<sup>2</sup> of the Bocas del Toro Province, on the coast of the Republic  
145 of Panama. It consists of a mosaic of wetland habitats, including the 80 km<sup>2</sup> Changuinola peatland, a domed peat swamp complex south-east of the Rio Changuinola (Phillips et al., 1997; Sjögersten et al., 2011; Troxler, 2007). Peat formation began around 4000–5000 years ago, with the shallowest deposits (~ 2 m) at the margins and the deepest (> 8 m) in the centre (Phillips et al., 1997). The area experiences a humid-tropical climate, with an average temperature of ~ 26 °C and annual precipitation of ~ 3000 mm (Phillips et al., 1997), with no pronounced wet or dry seasons (Phillips et al., 1997; Wright et al.,  
150 2013). The domed and largely ombrotrophic Changuinola peat swamp in Panama contains seven structured and roughly concentric vegetation communities (Phillips et al., 1997). In May 2019, we sampled four representative sites along a roughly SW-NE axis, broadly following the sampling stations established previously (Baird et al., 2017). The vegetation changes along this transect are driven by a strong nutrient gradient from the more mesotrophic outer regions towards the oligotrophic centre of the domes (Sjögersten et al., 2011; Troxler, 2007). Here we focus on two key vegetation endmembers: the mixed  
155 forest swamp phasic community (SSPS2: *Raphia taedigera* and *Camposperma panamensis*, Zone 4, 9°22'51.4"N 82°22'00.4"W), which features a relatively high availability of nutrients (Sjögersten et al., 2011); and the sawgrass community in the centre (SSPS4: *Myrica-Cyrilla*, Zone 1, 9°23'01.5"N 82°21'57.7"W), which is the most nutrient depleted of all the phasic communities (Sjögersten et al., 2011) and features dominantly *Cladium mariscus* and some stunted trees (Baird et al., 2017). SSPS2 was cored to 2 m deep, while SSPS4 was cored to the basement at ~ 5.4 m.

### 160 2.1.5 Mpologoma Swamp, Uganda

Mpologoma Swamp (UMp\_PA2; 0°57'53.3"N 33°44'31.3"E) is a papyrus swamp situated in Uganda, near the town of Tirinyi. The swamp is located on both banks of the Mpologoma river and encompasses a large area of ~ 12,195 km<sup>2</sup> as part



of the Kyoga Water management zone (Bunyangha et al., 2021). Due to its connectivity with the Mpologoma River, the site experiences high seasonal fluctuations in the water table. The vegetation is exclusively *Cyperus papyrus* (papyrus), with a mean average air temperature of ~ 20 °C. Mean annual precipitation is ~ 1220 mm with two distinct wet seasons in March–May and December–February (Chombo et al., 2018). Sampling was conducted along a 500 m transect away from the Mpologoma River. The core (2.35 m) included in this study is the central core of the transect, taken ~ 100 m from the River (Transect 2, point A). Sampling was carried out in July 2024, but despite occurring in the dry season, the water table level was about 80 to 100 cm above the peat surface.

### 170 2.1.6 Crymlyn Bog, Wales

Crymlyn Bog (UKCB; 51°37'54.3"N 3°53'48.3"W) is a lowland topogenous fen located at the eastern side of Swansea in Wales (UK) and is a Site of Special Scientific Interest. The vegetation at the coring location features mainly *Phragmites australis*, but *Cladium mariscus* and *Juncus spp.* are reported as well (Hughes and Dumayne-Peaty, 2002). In other parts of the fen, there is also *Betula* and *Salix* carr and several poor and rich stands, which range from *Sphagnum spp.* to *Typha/Cladium/Carex* dominated peat. Pore-water pH values measured at the time of sampling were ~ 6.2, which is broadly consistent with the previous literature (Hornibrook and Bowes, 2007). The near neutral pH is attributed to source water from Swansea valley percolating through calcareous rock. Annual precipitation (MetOffice Mumbles Head) between 1961–1990 was ~ 1000 mm. Coring was conducted in April 2025 using a Russian corer till the basement at 8.35 m, which extrapolates to an age of ~ 7,000-year BP following previously published age-models for this peatland (Hughes and Dumayne-Peaty, 2002).

### 180 2.1.7 Tor Royal, England

Tor Royal (UKTR\_1 & UKTR\_2; 50°32'08.4"N 3°58'15.5"W) is an ombrotrophic raised bog situated within Dartmoor National Park, South-West England (UK) (West, 1997). It is a designated Site of Special Scientific Interest because it features a relatively pristine plant community including *Sphagnum*, ericaceous shrubs, sedges and grasses reflecting raised bog conditions (Amesbury et al., 2008). Tor Royal has accumulated peat over the last ~ 6,000 years, with basement lying at 6.2 m at the centre of the dome (Charman et al., 1999). The water table depth is relatively stable at an average of ~ 30 cm below the surface. The mean annual temperature is 8 °C in the nearby town of Princetown (Burt and Holden, 2010). Annual precipitation is ~ 2,000 mm and relatively consistent across the year (Met Office, 2007). Our study includes a 1 m long core collected in April 2018 with a Russian corer from the centre of the dome (UKTR\_1) and a second, deeper core at 5.8 m collected in November 2024 (UKTR\_2).

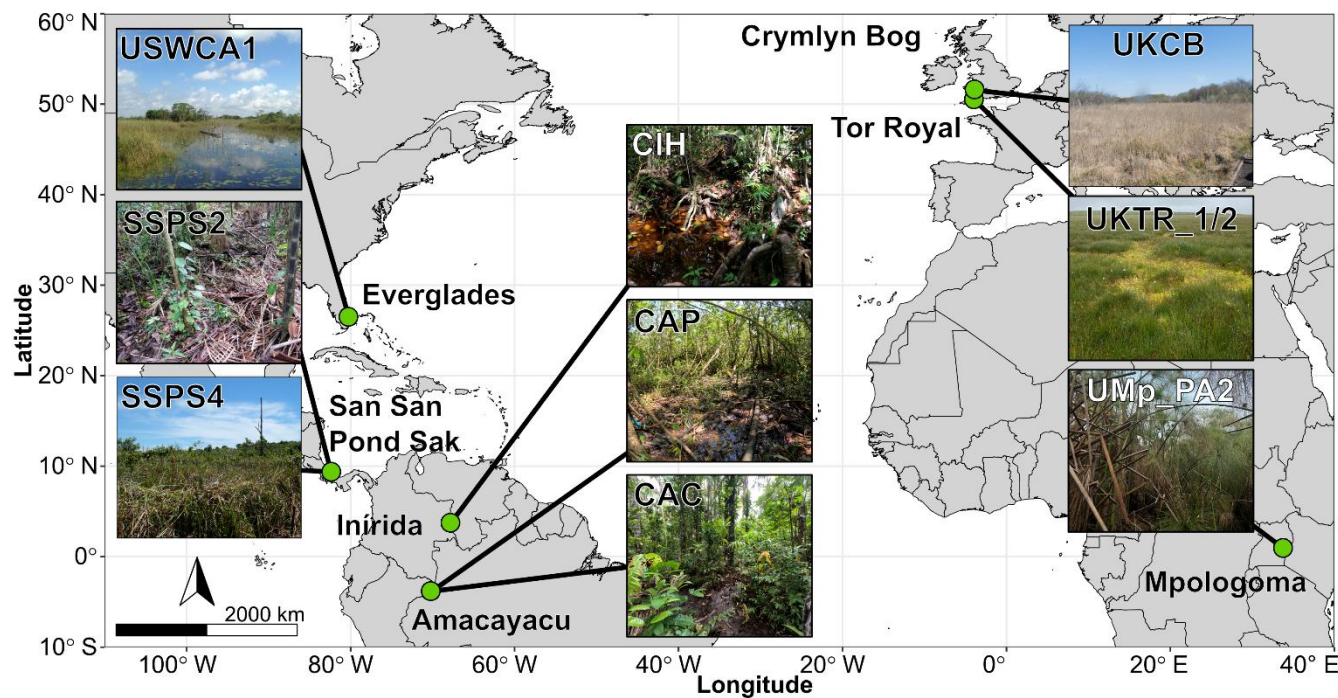


**Figure 1:** Map showing the location of the field sites along a global latitudinal transect. The map was made in R using Natural Earth publicly available data and the pictures were taken during the field campaigns.

## 2.2 Processing and bulk measurements

### 195 2.2.1 Sub-sampling & processing

All cores were kept at  $-20\text{ }^{\circ}\text{C}$  until subsampling. Sampling involved slicing each core into 1 cm sections, taking subsamples for bulk density/elemental analysis and pooling residual material into 5 cm integrated intervals. While slicing, great care was taken to maintain the heterogeneity of the tropical cores by cutting through large roots/wood detritus and pooling all material to obtain a representative sample of the peat at that depth. The samples were taken at higher resolution at the top of the profile since more microbial degradation was expected at the active peat surface. Litter samples were taken as grab bags of the surface and randomly subsampled for  $\sim 5\text{ g}$ . Plant material contains leaves and roots from 3–10 individuals to reach  $\sim 5\text{ g}$ , while trunk samples are from a single individual. The integrated peat, litter, and plant tissue samples were freeze-dried and subsequently homogenized into a fine powder using a Retsch MM400 Mixer Mill to obtain a homogenous representation of that sample.

205

Peat samples were solvent-extracted following a modified Bligh and Dyer procedure which involved six sequential sonication-assisted extractions using methanol, dichloromethane and phosphate buffer (2:1:0.8, v:v:v) for the first three and methanol and dichloromethane (2:1, v:v) for the second three. Litter and plant samples were extracted using a Microwave



210 Assisted Extraction system or ultrasonication using methanol and dichloromethane (2:1, v:v). The insoluble residues of peat and plant material, representing non-extractable macromolecules, were dried before further analyses.

### 2.2.2 Fourier transform infrared spectroscopy

215 FTIR assesses the solid-phase OM composition using the vibration of chemical bonds in it (Artz et al., 2006). Analyses were conducted using a PerkinElmer Spectrum Two FT-IR Spectrometer using ATR with 4 scans across a range of 4000-650  $\text{cm}^{-1}$  in duplicate. The spectra were processed *sensu* Artz et al. (2006), outputting a ratio of  $1030 \text{ cm}^{-1} / (1030 \text{ cm}^{-1} + 1506 \text{ cm}^{-1})$ , which was averaged from the duplicates and presented with 1 standard deviation as error bars (Fig. 2b). 1030  $\text{cm}^{-1}$  represents a signal from the C-O stretch in cellulose, while the 1506  $\text{cm}^{-1}$  represents a signal from aromatic ring stretching (Artz et al., 2006).

### 2.2.3 Total carbon and nitrogen

220 To acquire total organic carbon (TOC) contents for our peat samples, we weighed  $\sim 2$  mg of the freeze-dried, ball-milled and extracted residues in a tin capsule. The sample was analysed for elemental C & N with an elemental analyzer (EA) (vario PYRO cube; Elementar Analysensysteme GmbH, Hanau, Germany) calibrated with sulfanilamide (N: 16.26%, C: 41.81%). The precision as a relative standard deviation was  $< 5\%$  for both C and N. Peat typically does not contain carbonates that contribute to this signal; hence total carbon (TC) is interpreted as TOC (Chambers et al., 2011). Since the residues have undergone extraction, the values are named  $\text{TOC}_{\text{res}}$  to avoid confusion with common reporting of TOC on unextracted peat samples, but we expect  $\text{TOC}_{\text{res}}$  to be very similar to TOC as the mass of the extracted OM is an order of magnitude smaller than the bulk sample (Lehtonen and Ketola, 1993).

## 2.3 Pyrolysis – gas chromatography – mass spectrometry

### 2.3.1 Analytical standards

230 External standards were included in our analysis to contextualise our pyrolysate relative abundances; these include alkali-lignin (Sigma-Aldrich, CAS 8068-05-1) as a lignin standard, locust bean gum (Sigma, CAS 9000-40-2) as a hemicellulose standard, cellulose (Sigma-Aldrich, CAS 9004-34-6) as a cellulose standard, and solvent-extracted *Agave americana* (acquired from the University of Bristol Botanic Garden) residue (cutan) as an aliphatic standard (Deshmukh et al., 2005). To further constrain matrix/mixing effects, the commercial standards were mixed 1:1:(1) (*m/m(m)*) and included in our analyses.



### 2.3.2 Instrumental analysis

For almost all samples, approximately 0.5 mg of insoluble peat/plant residues and standard mixes were weighed into a pyrolysis tube. The exception was the Mpologoma (UMp\_PA2) peat samples, which required 5 mg to obtain a robust signal. Following this, the tubes were pyrolyzed for 20 s at 610 °C under a helium flow in a CDS Pyroprobe Model 6200. Pyrolysates were directly transferred at 310 °C onto a Thermo TRACE 1310 gas chromatograph with a split/splitless inlet (310 °C, 40 mL/min split flow, 1:40 split ratio) and either a Restek Rtx-1 column (60 m x 0.32 mm i.d.; 0.25 µm df; dimethyl polysiloxane) or an Agilent DB-1ms column (60 m x 0.32 mm i.d.; 0.25 µm df; fused silica). The GC oven was held at 40 °C for 4 min and ramped to 320 °C at 4 °C/min until a final hold at 320 °C for 10 min. Identification of pyrolysates was achieved with a Thermo ISQ 7000 mass spectrometer operating in full scan mode ( $m/z$  50-650, 5 scans/s, EI 70 eV) by mass spectral comparison with NIST and in-house pyrolysis product libraries in the Xcalibur software, as well as retention time/major ion comparison from published peat pyrolysis studies (Schellekens et al., 2009; Carr et al., 2010; McClymont et al., 2011; Klein et al., 2022). Most pyrolysis products were integrated using the Quan browser function in Xcalibur in the products' respective major extracted ion chromatogram (e.g. 4-Vinylphenol in EIC  $m/z$  120; see Table S1), with the exception of acetic acid, levoglucosan, levomannosan, and levogalactosan which required manual integration in the  $m/z$  60 mass trace. All automated integrations and identifications were checked manually to account for retention time shifts/misidentification. Every 12 samples, we ran the same sample again (SSPS2 4–7 cm) to ensure consistency and quantify the analytical error (Table S3).

### 2.3.3 Py-GC-MS statistical analysis

Prior to statistical analysis, all pyrolysate peak areas were converted to fractional abundance by dividing their respective peak area (derived from their specific unique  $m/z$  trace) by the total peak area of all. To untangle the dominant signals that govern the pyrolysis product abundances in peat and vegetation, we undertook principal component analysis (PCA) and Hierarchical Cluster Analysis (HCA) using R Statistical Software (R Core Team, 2025). Before conducting the analysis, we applied a min-max normalization per compound in all analysed samples excluding the standard mixes for PCA and HCA. Normalization equalizes the statistical variance for every compound, since properties of this workflow (instrument type, pyrolysis efficiency, ionization efficiency, ionization fragmentation pattern, and peak shape) prohibits absolute abundance elucidation (Klein et al., 2020). HCA was performed using the ward.D2 linkage on a Euclidean dissimilarity matrix and visualized using a dendrogram (Fig. 5). Branching in the dendrogram was investigated *ad hoc* by conducting paired t-tests between clusters and summarizing the pyrolysates with the lowest p-values manually. Ternary diagrams were constructed by taking a second order fractional abundance over the complete min-max normalized data including only groups of interest, such as lignin (G+S), Polysaccharides (Ps), Cellulose (Ce), and/or Aliphatics (Al). The pyrolysis-GC-MS-based polysaccharide / (polysaccharide + aromatic) ratio (PPA) was calculated by grouping peak areas functionally (Ps and Ce for polysaccharides and P, G, S, Ca and Ar for aromatics).

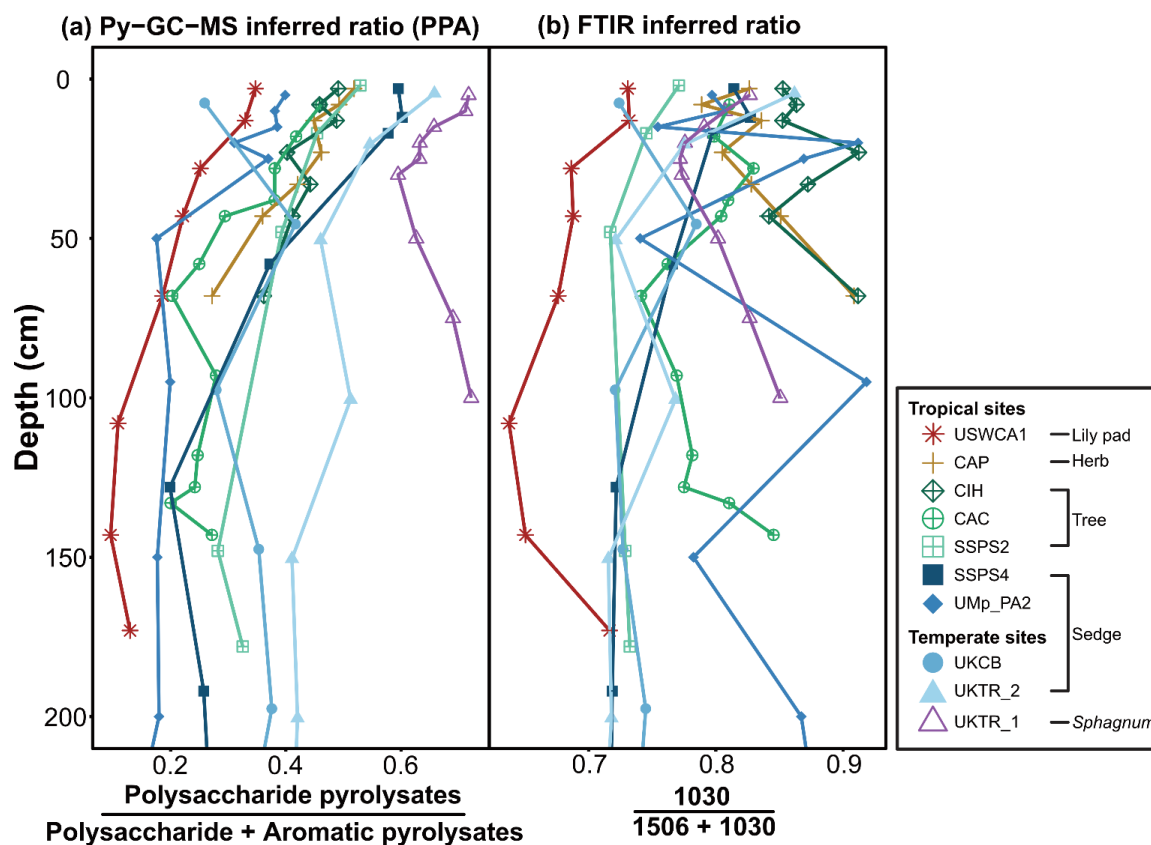


### 3 Results & Discussion

#### 3.1 FTIR shows silicate bias in lowland tropical peatland systems and py-GC-MS is more applicable

270 FTIR analyses reveal clear differences in carbohydrate to aromatic carbon ratios among the study sites as well as with depth (Fig. 2b). In SSPS (Panama), our FTIR data is consistent with the published work of Upton et al. (2018), with SSPS2 having a high aromatic character arising from its lignin-rich forest cover and SSPS4 being more carbohydrate-rich reflecting the sawgrass vegetation. Both sites become more aromatic with depth. Our other sites partially fit these observations. The Everglades peat has low carbohydrate contents, perhaps reflecting a highly degraded character arising during transport and

275 burial in this perpetually flooded site. In contrast, Cananguchal (*Mauritia* palm dominated) and Tor Royal (*Sphagnum*) have elevated carbohydrate contents, similar to that of SSPS4. However, FTIR analyses suggest that Mpologoma (papyrus swamp), Pantano (herbaceous swamp) and Inírida (hardwood swamp) all have high and very variable apparent carbohydrate contents.

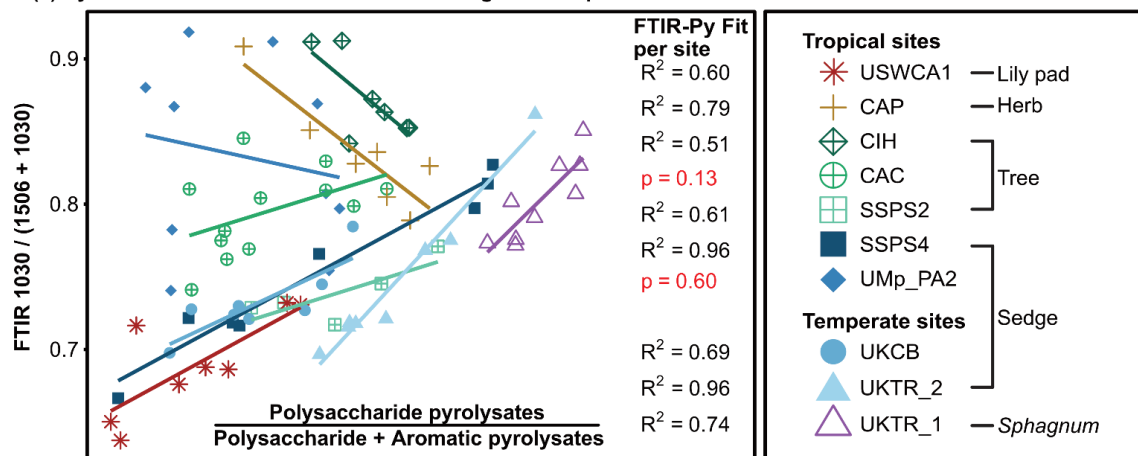


280 Figure 2: (a) Downcore plot of the py-GC-MS-based PPA (polysaccharide pyrolysates / (polysaccharide pyrolysates + aromatic pyrolysates)). (b) Downcore plot of the FTIR-based 1030/(1030+1506) ratio where 1030 cm<sup>-1</sup> represents the C-O stretch in cellulose, while 1506 cm<sup>-1</sup> represents the aromatic ring stretching.

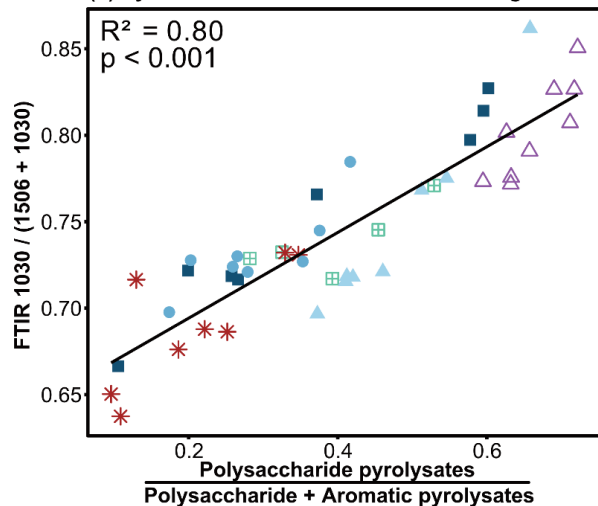


285 We compared these FTIR data to a py-GC-MS-derived polysaccharide pyrolysates / polysaccharide pyrolysates + aromatic pyrolysates ratio (PPA; Fig. 3a). Generally, SSPS2, SSPS4, the Everglades, Crymlyn Bog, and both Tor Royal cores also follow similar downcore trends to the functional Py-GC-MS based ratio (Fig. 3b,  $R^2 = 0.80$ ,  $p < 0.05$ ). However, Cananguchal, Mpologoma, Pantano, and Inírida show either no correlation between the two ratios ( $p > 0.05$ ) or a negative correlation in the case of Pantano and Inírida, and FTIR analyses suggest much higher carbohydrate percentages (Fig. 3a).

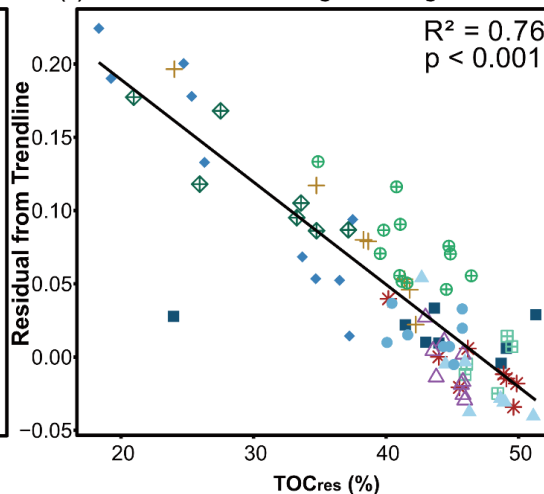
(a) Py-GC-MS vs FTIR Ratio with Pearson regressions per site



(b) Py-GC-MS vs FTIR Ratio of sites with good fit



(c) Residual from linear regression against TOC<sub>res</sub>



290

295

Figure 3: (a) Cross plot between the FTIR-based and py-GC-MS-based ratios with a linear regression (Pearson) per site. The goodness of fit by  $R^2$  is reported per site showing sites where FTIR and py-GC-MS ratios agree. (b) Linear regression (Pearson) on sites that show little silicate mineral interference (USWCA1, SSPS2, SSPS4, UKCB, UKTR\_2, and UKTR\_1) between the FTIR-derived ratio and py-GC-MS derived ratio. (c) Linear regression (Pearson) on the residual (FTIR dimension) from the regression in panel b against total organic carbon ( $TOC_{res}$ ). Likely silicate mineral bias is also introduced in  $TOC_{res} > 40\%$  peat material, making tropical sites seem more carbohydrate-rich in FTIR than derived from py-GC-MS.



FTIR has known limitations regarding silicate mineral interference, which creates a peak at  $\sim 1030 \text{ cm}^{-1}$  that overprints the carbohydrate band (Reig et al., 2002). Therefore, the anti-correlation between the two functionally defined ratios at Pantano and Inírida (Fig. 3a) likely indicates increased (silicate) mineral content at depth. This is consistent with the lower  $\text{TOC}_{\text{res}}$  at these sites at depth ( $< 30 \text{ wt.}\%$ ) and visual observations while coring/subsampling. Further confirming this interpretation, the offset between the FTIR-based ratio in the Colombian sites and Mpologoma from the linear relationship derived from the FTIR-based and pyrolysis-based ratios elsewhere, is significantly correlated with  $\text{TOC}_{\text{res}}$  (Fig. 3c;  $R^2 = 0.76$ ,  $p < 0.05$ ), which represents the ratio between OM and other material in the core, likely (Si-rich) sediment from nearby rivers. Therefore, it appears that the application of FTIR could be inappropriate for dynamic tropical lowland settings that experience river flooding episodes that result in high and variable silicate mineral interference of the carbohydrate band. The strong linear relationship between the FTIR offset with  $\text{TOC}_{\text{res}}$  suggests that even at high TOC contents ( $>50 \text{ wt.}\%$ ), there is potential bias for silicate minerals to impact interpretations.

This highlights the utility of pyrolysis-GC-MS based ratios to determine OM alteration as this is not affected by silicate mineral interference. Previous work shows that peat pyrolysis-GC-MS characterization is consistent with data obtained using solid state  $^{13}\text{C}$  nuclear magnetic resonance (NMR) spectroscopy (Kaal et al., 2007; Schellekens et al., 2015), and both this and other work show that it agrees broadly with FTIR (e.g. Kim et al., 2026). Solid state  $^{13}\text{C}$  NMR does not suffer from direct silicate mineral interference because C is absent in silicates, but it does exhibit matrix effects (Freitas et al., 2002) and does not have the same biopolymer origin specificity that pyrolysis-GC-MS enables. Generally, all bonds characterized in solid state  $^{13}\text{C}$  NMR and FTIR are linked only indirectly to biomolecules enriched in that bond type. For example, a significant shift from hemicellulose to cellulose would not affect the proportion of O-alkyl bonds in  $^{13}\text{C}$  NMR, which reveals the ring oxygen of all polysaccharides (Normand et al., 2021; Moody et al., 2018). This can be detected in py-GC-MS by different proportions of levoglucosan, which is enriched in the pyrolysis of cellulose, against levomannosan, levogalactosan and several furan-containing pyrolysates (Schellekens et al., 2015). Although cellulose and hemicellulose are both polysaccharides and thus have the same “labile” assignment in modelling efforts (Chadburn et al., 2022; Young et al., 2021), their ratio as determined through py-GC-MS is an important explanatory variable in the microbial community structure between stages of recovery post-degradation in a Welsh peatland (Ring-Hrubesh et al., 2025).

However, caution is still required in interpreting pyrolysis-GC-MS in terms of peatland OM character, as it is inherently non-quantitative; often a high percentage of carbon will not be mobilised and left behind as char under ideal flash pyrolysis conditions ( $48.4 \pm 5.5\%$  of C) (Klein et al., 2020), and pyrolysates can exhibit differences in response factors (Kaal et al., 2007). Matrix effects can also occur during pyrolysis (Alcaniz et al., 1989), such as shifting pyrolysis products of free alkanolic acids/alcohols in the presence of clay (Nierop and Van Bergen, 2002). This specific effect is not relevant to our study, since these compounds were extracted prior to pyrolysis, but similar clay interference might be expected for aliphatic



330 macromolecules. However, pyrolysis-GC-MS does allow the investigation on the chain-length distribution of these aliphatic  
pyrolysates, which can aid source-allocation more accurately than FTIR or NMR.

### 3.2 Vegetation leaves a signature in the peat OM, even when decomposition transforms the OM significantly

#### 3.2.1 Py-GC-MS characterization of peat reveals decomposition and vegetation signature while peat-forming 335 vegetation is characterized by tissue and plant group

Pyrolysates of peat ( $n = 83$ ) and plant ( $n = 61$ ; Table S2) samples contain all the groups and compounds (Table S1) that have  
been identified in comparable literature (Schellekens et al., 2012; Schellekens et al., 2015; Klein, 2022; McClymont et al.,  
2011; Carr et al., 2010). Specifically, 143 pyrolysates are detected, integrated, and assigned into structurally distinctive  
groups with similar origin. This includes the lignin monomer groups (Schellekens et al., 2009; Hedges and Mann, 1979):  
340 phenols (P,  $n = 12$ ), which can be derived from *p*-coumaryl lignin monomers or other polyphenol sources; guaiacols (G,  $n =$   
 $16$ ), which are from coniferyl lignin monomers; syringols (S,  $n = 17$ ), which originate from sinapyl lignin monomers; and  
catechols (Ca,  $n = 4$ ), which occur naturally in lignin and tannins (Galletti and Reeves, 1992). Furthermore, we detect  
aromatics (Ar,  $n = 17$ ) from miscellaneous aromatic macromolecules and polysaccharides (Ps,  $n = 22$ ), mostly from (hemi)-  
cellulose plant components; levoglucosan (Ce,  $n = 1$ ), which preferentially occurs in cellulose (Shafizadeh and Fu, 1973);  
345 nitrogen-containing compounds (N,  $n = 7$ ) which occur in plants but the variance in peat is mostly attributed to  
microbial/fungal biomass i.e. proteins (Klein, 2022); and lastly, aliphatic compounds (Al; *n*-alkanes,  $n = 23$  and *n*-alkenes,  $n$   
 $= 24$ ), which originate from either aliphatic macromolecules in higher plants (Buurman et al., 2006; Schellekens et al., 2009;  
Schellekens and Buurman, 2011; Schellekens et al., 2012) or condensation of soluble aliphatic biomolecules (Gupta et al.,  
2006). Major peaks in our chromatograms (Fig. A1) that represent lignin include the phenols (4-Vinyl (P3)/4-Methyl (P2)  
350 phenol (P1)), guaiacols (4-Vinyl (G3)/4-Methyl (G2) guaiacol (G1)), and syringols (4-Vinyl (S3)/4-Methyl (S2) syringol  
(S1)). The dominant polysaccharides are furfural, levogalactosan, levomannosan & levoglucosan, and the aliphatics are  
represented by *n*-alk-1-ene/*n*-alkane doublets ranging from  $C_9$  to  $C_{31}$  in length.

To assess whether pyrolysates attributed to each macromolecular assignment exhibit similar trends, we explored their  
355 variance using PCA on both the peat and plant dataset as well as the combined dataset. The full dataset PCA resulted in  
PC1–4 together accounting for 64.1% of the variance (Fig. A2). Pyrolysates grouped into their respective macromolecular  
assignments (aliphatic, lignin and polysaccharide) at similar loading angles, independently confirming their macromolecular  
origin. The plant samples group closely together in the biplot, because their variance is smaller compared to that of the peat  
(paired t-test;  $p < 0.002$ ). Variance within the plant subset ( $n = 61$ ; Table S2) reflects a combination of taxonomic origin and  
360 tissue type and shows distinct behaviour in its separate PCA. Below, we first describe the variation and major groups in the  
vegetation (including leaf litter) and then expand that analysis to compare vegetation to peat composition.

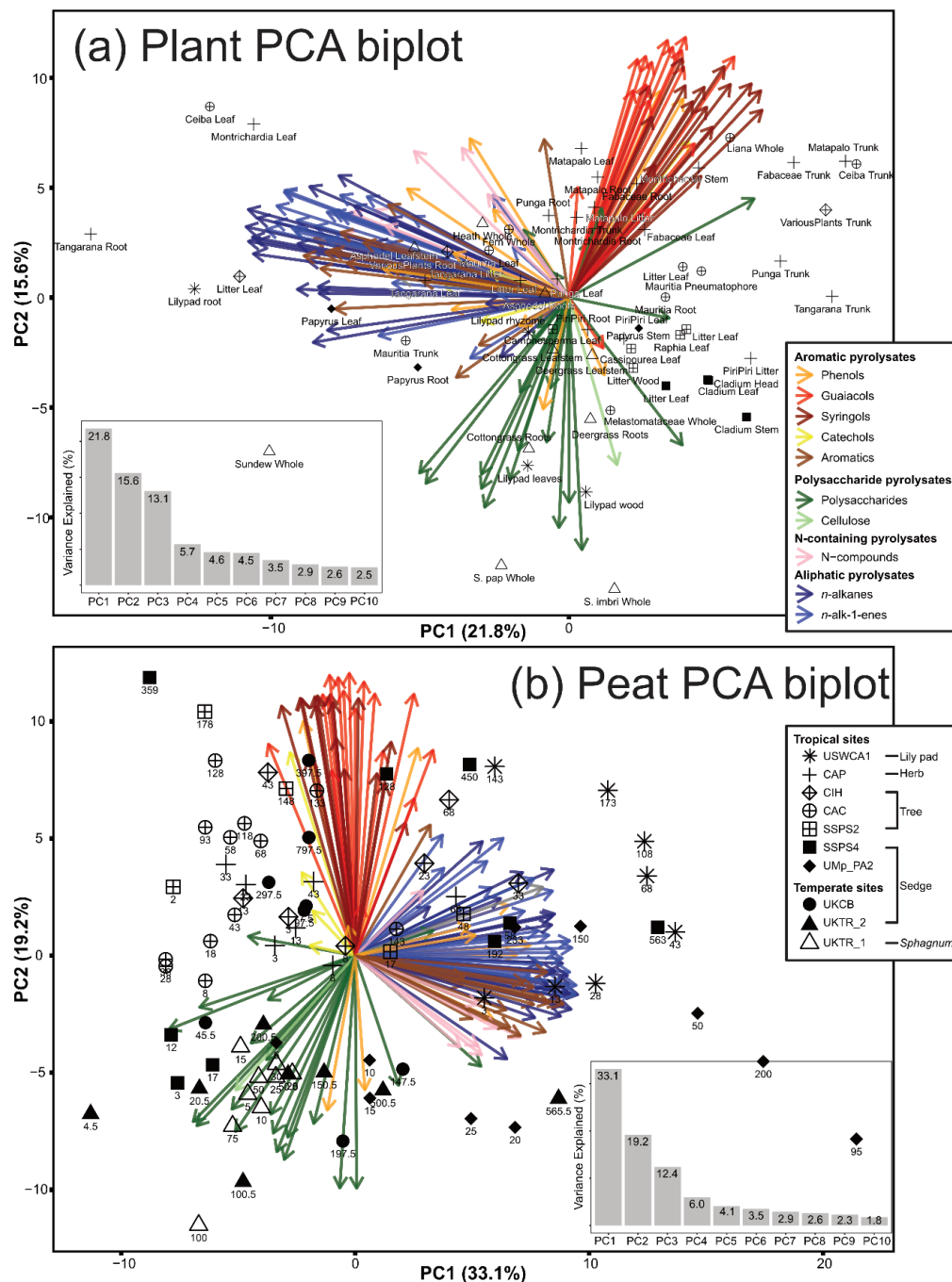


Figure 4: (a) PCA biplot showing main controls of the plant dataset with pyrolysate vectors coloured by macromolecular assignment and shape by site of origin. The text features the colloquial name of the plant (detail in Table S2) and tissue type analysed. A bar chart in the bottom left features the PC scores. (b) PCA biplot showing main controls of the peat dataset with pyrolysate vectors coloured by macromolecular assignment and shape by site. The text features the depth the peat originates from. A bar chart in the bottom right features the PC scores.

365



The plant and litter pyrolysate abundance variance is predominantly explained by principal components 1–3 (21.8%, 15.6% and 13.1%, respectively), and subsequent PC scores drop under 6% (Fig. 4a). The pyrolysates group similarly as in the full  
370 dataset, but plant samples exhibit distinct groupings based primarily on tissue type and secondarily on broad taxonomy (i.e. grass, herb, tree). The aliphatic components primarily load onto PC1. These are absent in many of the trunk tissue samples, such that a cluster of trunk tissue samples is apparent on PC1 (positive loading). Leaves and roots generally contain more aliphatic components, with a strong negative PC1 loading. Leaf aliphatic components could derive from either cutan (Boom et al., 2005) or residual plant waxes, the latter being consistent with higher abundances of the C<sub>29</sub> and C<sub>31</sub> *n*-alkanes  
375 encapsulated in the leaf cuticle, preventing their extraction (Gupta et al., 2006). The aliphatic macromolecules found in root material are from suberan (Nierop, 1998). PC2 shows a clear distinction of lignin-derived pyrolysates (positive loading) from polysaccharides (negative loading) (Fig. 4a). The *Sphagnum* species from Tor Royal plot negatively on PC2 due to the absence of G/S-lignin and a variety of diagnostic polyphenol pyrolysates universal among *Sphagnum* (Van Der Heijden et al., 1997). The trunk group plots positively, represented by a higher proportion of guaiacol and syringol lignin. Other plants  
380 and tissues exhibit varying PC2 scores, apparently reflecting the balance of lignin and polysaccharides and is discussed in greater detail in Section 3.3.1. PC3 primarily reflects the behaviour of specific polysaccharides, phenols and aromatic compounds as a positive loading, and specific phenols and aliphatics as negative loadings (Fig. A3). Crucially, this axis separates the hardwood tree samples from the herbaceous and palm samples by enrichment of syringols in hardwoods and phenols in softwoods. Together the PCA on the plant samples indicates that tissue and plant type are the main controls on  
385 plant and hence peat input OM content. Next, we assess this in the peat material itself.

The majority of total variance in the peat dataset is explained by PC factors 1–4 (70.7%), where PC1 (33.1%) is described by positive loadings of polysaccharide pyrolysates and negative loadings of aliphatics (*n*-alkanes & *n*-alkenes), aromatics and N-compounds (Fig. 4b). N-compounds occur naturally in plants but are quickly degraded and can be pyrolysis products of  
390 amino-acids in proteins (e.g. diketodipyrrole; Stankiewicz et al., 1996). Therefore, N-compounds can act as a proxy for microbial/fungal necromass in peat (Kaal et al., 2017). PC2 (19.2%) mostly features positive loadings of guaiacols, syringols and catechols derived from G and S lignin (Hedges and Mann, 1979) and negative loadings of different polysaccharide pyrolysates. Polysaccharide-related compounds include several oxygen-containing heterocycles such as furans, likely originating from pentoses (e.g. xylose) found in hemicelluloses (Moers et al., 1990). Other common heterocycles are  
395 levomannosan, levogalactosan and levoglucosan, which are pyrolysis products of the monosaccharides mannose, galactose and glucose, respectively (Klein, 2022). Levoglucosan has been applied in peatland studies as a marker for a higher proportion of cellulose as cellulose is built up exclusively from glucose monomers (Schellekens et al., 2009). PC3 (12.4%) features positive values from aromatics, primarily those not directly associated with lignin. Some of these, such as naphthalene and fluorene, can form through pyrogenic events (Schellekens et al., 2009), but other monocyclic compounds  
400 that group similarly can have diverse sources, such as simpler polyphenols (Schellekens, 2013). We suggest that these compounds reflect the breakdown of more complex aromatic-hosting compounds. Negative values on PC3 are attributed



mostly to polysaccharides. PC4 (6%) has loadings that split the alkanes from the alkenes, which hints at an entrenched leaf wax signal (Schellekens and Buurman, 2011).

405 Generally, most compound group associations show loadings that are grouped according to inferred biomolecular origin, such as the aliphatic compounds, guaiacols, syringols, polysaccharides, and N-compounds. However, phenols (P) are scattered in positive and negative PC2 loadings, which indicates that they are, in this dataset, not representative of one uniform pool. Phenols can originate from *p*-coumaric lignin but have been found as a *Sphagnum* biomarker (*p*-isopropenylphenol; Boon et al., 1986) and as a graminoid indicator (4-vinylphenol; Saiz-Jimenez and De Leeuw, 1986).  
410 Therefore, when further discussing lignin in this paper, we include only guaiacol and syringol pyrolysates, while considering the diverse origin of phenols.

Tor Royal and the Everglades are the only sites that group relatively tightly in the PCA1–2 plot. Tor Royal is characterised by negative loadings on PC1 and PC2, similar to the polysaccharides. However, the deeper Tor Royal samples exhibit an  
415 increase in PC1 likely driven by aliphatics. The Everglades has negative loadings on PC1 and positive loadings on PC2, similar to the aliphatic and lignin-derived components. In contrast, each of the other tropical sites exhibits a wide spread in the PCA1–2 plot, arising from great variance within the peat with depth. This primarily reflects a general decrease of PC1 and increase of PC2 at depth, with peat becoming enriched in aliphatics and lignin. This likely represents peat decomposition at depth, which is common in peat pyrolysis studies (Ryan et al., 1987; Schellekens et al., 2015). Our work now shows that  
420 this transformation is remarkably uniform across this diverse set of tropical sites. PCA3–4 group samples based on sites, therefore representing the vegetation fingerprint left in the peat OM, even at depth (Fig. A3b).

In summary, our analyses of the peat material itself indicates that preferential degradation and type of dominant vegetation are the main drivers of peat macromolecular compositions, with a stronger preferential degradation signal in the tropical  
425 sites. Next, we further explore the source vegetation fingerprint on the peat OM and assess whether this fingerprint is consistent and persistent at depth and between vegetation and peat through cluster analysis.

### **3.2.2 Cluster analysis on the macromolecular composition of peat and peat-forming vegetation reveals that plant macromolecular composition is retained in all peat horizons**

430 Overall, the vegetation PCA shows a dominant axis of variance based on the lignin and aliphatic macromolecules, whereas the variance in polysaccharides drives the peat ordination. However, PCA assumes linearity, while HCA is based on distance matrix that is more suited for specific pyrolysate signatures of plant species (James et al., 2013). Therefore, we applied HCA to the integrated peat and peat-forming vegetation database to explore further the chemotaxonomic fingerprints left by the vegetation on the peat composition and OM characteristics. The HCA dendrogram (Fig. 5) shows a major cluster of peat



435 samples that is characterized by high proportions of aliphatic components, and a less aliphatic (and furan-rich) cluster of peat  
that is further split through differences in lignin monomers and polysaccharide abundances, creating sub-clusters dominated  
by *i*) G-lignin, *ii*) N-compounds and *iii*) polysaccharides. The plant samples are mostly characterized by an absence of  
aliphatic pyrolysates and cluster separately into sub-clusters dominated by *i*) hemicellulose, *ii*) vinyl-phenol (P3), *iii*) S-  
lignin, *iv*) P-lignin, *v*) G-lignin, and *vi*) phenols, which for the most part map onto plant groups with a clear chemotaxonomic  
440 consistency. Below we describe the defining characteristics of each of the clusters described above for the plants first and  
link the chemotaxonomic fingerprint on the peat to the vegetation clusters.

Most plant samples are characterized by a low proportion of aliphatics, leading to a clear divide between plant and peat  
samples in the HCA dendrogram (Fig. 5). Further branching results in the vegetation being divided into six diagnostic  
445 clusters. One of these is a polysaccharide-rich cluster which contains *Sphagnum papillosum*, *Sphagnum imbricatum*, sundew,  
and several lily pad tissues. These plants are known for their low/absent lignin content (Weng and Chapple, 2010), and they  
are the dominant species in Tor Royal and Everglades sites (see section 2.1).

Another cluster is defined by a higher proportion of 4-vinylphenol (P3) and contains all sedge species, regardless of plant  
450 tissue type, i.e. roots, stems and leaves. 4-Vinylphenol is a known biomarker for sedges in peat (Schellekens et al., 2015), as  
well as grasses in general (Saiz-Jimenez and De Leeuw, 1986), but we here show that this extends to tropical species, such as  
Papyrus roots and stems, and Piri Piri. This cluster also includes some shallow samples of SSPS4 and UKTR\_2 peat,  
suggesting that this part of these peatlands consists primarily of unaltered sedge material. Intriguingly, none of the  
Mpologoma peats, where papyrus is the sole plant species, groups with this cluster. The primary reason for this is the  
455 enrichment of aliphatics in this papyrus peat, even at shallow depths (Fig. 6a).

G and S lignin is the critical factor in defining the other four plant clusters. A diagnostic S-lignin dominated cluster is present  
which contains most trunks of eudicot trees included in our study, consistent with S-lignin being characteristic for woody  
tissue (Hedges and Mann, 1979). Intriguingly, two depths from Panama are also found in this cluster. SSPS is known for  
460 containing larger wooden detritus in cored sections, even at SSPS4, which experienced a past vegetation change from a  
community more akin to that at SSPS2 to the current *Cladium*-dominated cover (Phillips et al., 1997). These depths appear  
to have retained a wood signal in their bulk OM composition, highlighting the long-lasting impact of a high contribution of  
wood to peatlands.





470

Palm material splits off into a cluster with a hemicellulosic and phenol-rich character, which is consistent with the softer nature of its wood and the dominance of P-lignin in palm species (Hoyos-Santillan et al., 2016). This cluster features most *Mauritia* tissues, *Raphia*, and litters from SSPS2 and Cananguchal, which are all palm tissue or litters from palm-dominated sites. The top 40 cm of the Cananguchal peat also features in this cluster, confirming the dominance of fresh palm material at 475 40 cm depth likely arising from the extensive pneumatophore system of *Mauritia flexuosa*.

480

The third G and S balanced lignin sub-cluster has a higher proportion of hemicellulose and guaiacol pyrolysates and is represented by miscellaneous plant leaves and roots from globally dispersed sites. Only the surface (2 cm) sample from SSPS2 clusters with these plants, probably reflecting a larger contribution of *Camposperma* leaves or understory rather than *Raphia* palm material.

485

The hemicellulose-enriched cluster also contains abundant N-compounds and defines the top 30 cm of the Mpologoma Papyrus swamp, whereas the deeper Mpologoma samples group in the aliphatics cluster discussed below. The main difference between these depth intervals arises from an enrichment of hemicelluloses in the surface and an enrichment of phenols and high molecular weight (HMW) *n*-alkanes at depth. This suggests that a shift in the dominant Papyrus plant tissue is reflected in the overall peat composition: the surface is dominated by the more labile, N-compound rich Papyrus roots and the deeper peat is dominated by Papyrus leaves which have a phenolic character, which is counterintuitive given current models of tropical peat accumulation (Chimner and Ewel, 2005).

490

The lignin-enriched cluster of peat includes most of the samples from Crymlyn Bog, Cananguchal, Pantano, and Inírida. These peat samples are enriched in lignin but otherwise have a characteristic pyrolytic fingerprint. Further branching in this cluster is associated with phenolic enrichment for the Crymlyn bog and Cananguchal peat, which likely reflects the phenolic character of sedges and palms, respectively. In contrast, the Pantano/Inírida subgroup features a more aliphatic and cellulose-rich character, perhaps caused by the preferential degradation of hemicelluloses (Van Der Heijden and Boon, 1994; Hedges et al., 1985). The larger aliphatic cluster features peat samples from the Everglades, Panama, Inírida, and deeper Mpologoma peat, and indicates increased decomposition in these peats. All of these are from (deep) tropical swamp peatlands and are also highly aromatic and aliphatic in character. The strong aliphatic character of the Everglades samples is likely caused by extensive degradation of plant material due to permanently high water table and the high abundance of aliphatics in lily pad root material. Another indication that degradation is an important factor in this cluster is the higher proportion of cellulose 495 500 caused by the preferential degradation of hemicelluloses (Hedges et al., 1985).

To summarize, the clustering of peat and plant samples in our HCA further demonstrates that the macromolecular composition contains a fingerprint that inherently links peat to the source vegetation. While the PCA features a convergence



of pyrolysate variance at depth, the subtle differences highlighted in the HCA indicate that the original plant material leaves a persistent fingerprint in the peat OM. This fingerprint persists regardless of its degree of degradation and likely influences the peat recalcitrance to microbial degradation and carbon cycle dynamics, even 1,000s of years after peat formation. Next, we elucidate the source and enrichment of aliphatics in the peat material, which forms the biggest discriminant between vegetation and peat material.

### 3.2.3 Aliphatic compounds are enriched in peat and signal early degradation

Aliphatic pyrolysates form the primary discriminant in our statistical analysis, represented through PC1 (Fig. 4) and the first two branches of our HCA dendrogram (Fig. 5). An enrichment of these aliphatics defines all peat samples in our database, which includes a range of tropical peatlands as well as a temperate fen and bog. These aliphatics could be produced by the condensation of biological alkyl compounds, such as *n*-alkanes, fatty acids, or alcohols into a larger macromolecule during humification (Lichtfouse et al., 1995), or the selective preservation of larger aliphatic-rich macromolecules such as cutin, cutan, or suberan (Deshmukh et al., 2005; Nierop, 1998; Gupta et al., 2006; Gupta et al., 2007b). The *n*-alkane/*n*-alk-1-ene ratio is close to 1 in most of our plant and peat material, especially from C<sub>16</sub> to C<sub>18</sub> (Fig. 6b). This suggests that the *n*-alkane/alk-1-ene doublets originate from pyrolytic cracking (Schellekens and Buurman, 2011). However, the *n*-alkane/*n*-alk-1-ene ratio in the HMW doublets increases and exhibits a subtle odd-over-even distribution (*n*-alkane/alk-1-ene ratio ~ 2) in the chain length (Fig. 6b). This suggests a contribution of non-extractable, entrained or bound leaf waxes released through volatilization of odd *n*-alkanes or even decarboxylation / dehydration of fatty acids/alcohols (Nierop and Van Bergen, 2002; Eglinton and Hamilton, 1968). The *in-situ* condensation mechanism is unlikely to be at play given the abundance of aliphatic macromolecules at the peat surface and the high temperatures (>300 °C) required to significantly produce condensed aliphatic macromolecules (Gupta et al., 2007a; Stankiewicz et al., 2000). Furthermore, although the distribution in plant samples is variable, both peat and plants have a similar pattern among the HMW components and both feature a higher proportion C<sub>14</sub>/C<sub>15</sub> *n*-alkane/*n*-alk-1-ene doublets, probably derived from cutin, which is common in plants (Schellekens and Buurman, 2011).

Even the shallowest peat is enriched in aliphatic components, which implies that plant material undergoes degradation before entering the peat horizon or in early diagenesis, enriching the proportion of the aliphatic macromolecules relative to polysaccharides and lignin. Aliphatic macromolecules are energetically difficult to break down, either aerobically or anaerobically (Gunina and Kuzyakov, 2022; Lorenz et al., 2007), which explains their preferential resilience. We also detect more aliphatics with increasing depth in some peat (Fig. 6a), which suggests that such preferential degradation persists under anaerobic conditions, although the mechanisms could differ among sites. In the Everglades, aliphatic pyrolysates are particularly abundant, both at the surface and significantly enriched at depth ( $R^2 = 0.67$ ,  $p < 0.05$ ). The lily pad roots feature a high proportion of aliphatics, making them a likely source for the aliphatics detected in these peat samples. The Everglades



540 site is also permanently inundated, such that significant aerobic degradation could have happened during transport and  
sinking, prior to reaching anoxic conditions in the peat profile. The Mpologoma papyrus swamp also contains a high  
proportion of aliphatics (up to 60% akin to *A. americana*), but especially at depth (<50 cm), which is likely sourced from the  
aliphatic-rich Papyrus leaf and subsequent aerobic and anaerobic degradation enrichment (Fig. 6a). The deeper Tor Royal  
core (UKTR\_2) also shows a significant enrichment of aliphatics at depth ( $R^2 = 0.82$ ,  $p < 0.05$ ), but it is more enriched than  
any measured plant litter, suggesting a continuous anaerobic preferential preservation of these aliphatic macromolecules  
(Schellekens and Buurman, 2011). The proportion of aliphatics at other sites, however, does not increase with depth (Fig.  
6a), suggesting that their aliphatic enrichment relative to the peat-forming plants was caused by aerobic degradation prior to  
545 deposition or during the earliest stages of degradation.

Regardless of the mechanisms, the aliphatics are the result of early diagenesis and therefore represent a large proportion of  
the peat macromolecular signal, which could be an underappreciated recalcitrant carbon pool. In the next section we dissect  
the effect of downcore degradation on plant biopolymers.

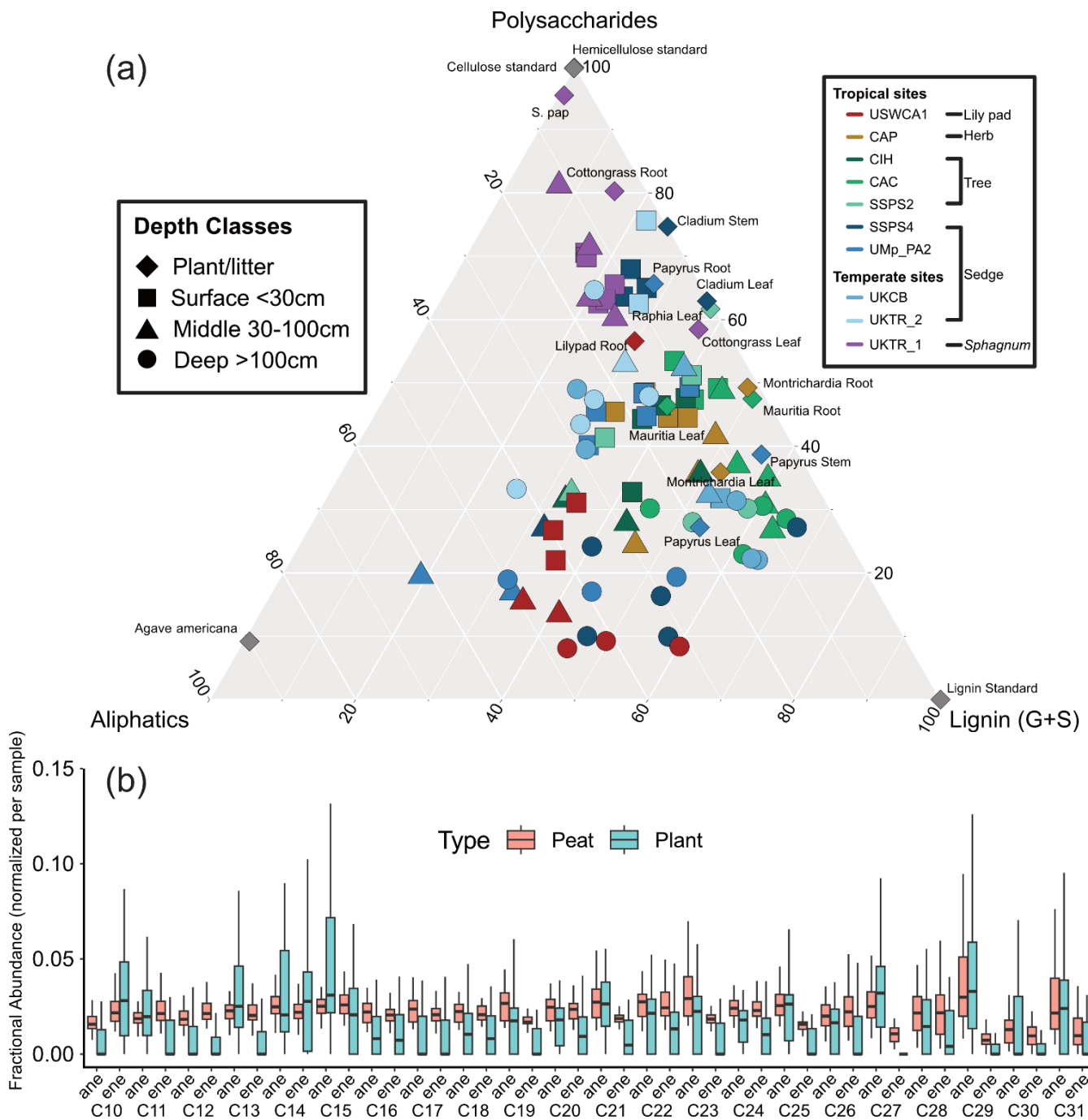


**Figure 6:** (a) Ternary diagram showing the pyrolytic fingerprint similarity (%) between important plant tissues, peat, and external analytical standards. (b) Boxplot showing the fractional abundances within the aliphatics observed in both the plants and peat dataset among different chain lengths (C10-C31) of n-alkanes (ane) and n-alk-1-enes (ene). The lines show the min-max values, while the box is between the first, second and third quartile.



### 555 3.3 Macromolecular composition of peat alters to recalcitrant composition at depth with implications

#### 3.3.1 Plant biopolymers show consistent downcore anaerobic preferential degradation of polysaccharides

Most carbon in peatlands originates from (dead) vegetation which on a molecular level is built primarily from three widespread biopolymers that give structure to the cell walls; cellulose, hemicellulose, and lignin (Scheller and Ulvskov, 2010). To compare the proportion of these biopolymers among the peat-forming vegetation and associated peat and trace  
560 how they change downcore, we pooled pyrolysates associated with these biopolymers and normalized their proportion with analytical standards. The percentages arising from these assignments are not quantitative and should be considered as a percentage relative to a purified standard. For example, a 30% proportion of hemicellulose does not suggest 30% weight percentage of the biopolymer pool is made up from hemicellulose, rather that the pyrolysis profile is 30% similar to hemicellulose. For the remainder of this section, macromolecule percentages refer to the percentage in  
565 lignin/cellulose/hemicellulose space.

In our dataset, most of the major peat-forming vegetation have a pyrolytic profile characterized by  $\sim 40 \pm 5\%$  lignin,  $\sim 40 \pm 4\%$  hemicellulose and  $\sim 20 \pm 5\%$  cellulose ( $\pm$  Standard deviation from Table S3; Fig. 7a). However, the range is large, with the most lignin-enriched plant being the papyrus leaves that contained 64% lignin. On the other hand, *Sphagnum*  
570 *papillosum/imbricatum* contained 0% lignin. Surface peat samples of the tropical sites have distributions comparable to those of the vegetation, but at depth the lignin associated pyrolysates become strongly enriched, with samples such as SSPS4 at 450 cm and USWCA1 at 143 cm having a pyrolytic profile 85% like lignin. This shift cannot be attributed exclusively to differences in past vegetation, because the lignin percentage exceeds values observed in any modern peat forming  
575 vegetation. Instead, these downcore changes reflect profound alteration of the biopolymer composition through preferential breakdown of polysaccharides relative to lignin at depth. Although the trend towards increasing lignin proportions is universal in our dataset, each site exhibits specific patterns, reflecting the interaction of preferential biomolecule degradation, differential plant tissue preservation and past vegetation change as discussed below. The following sections discuss the macromolecular composition of each site ordered on their dominant vegetations as each site and vegetation exhibits nuances.

580 The Everglades peat core consists primarily of lily pad detritus, but this is not directly reflected by the OM composition. The surface peat is  $\sim 50\%$  lignin, whereas the lily pad tissues are polysaccharide-rich with only  $\sim 20\%$  lignin. This, in combination with the high proportion of aliphatics, likely derived via selective enrichment of aliphatics in lily pad fine roots; see section 3.2.3, suggests that the OM has undergone significant aerobic degradation prior to becoming peat. Nonetheless, the peat profile in the Everglades features a continued enrichment of lignin at depth, transforming from the  $\sim 50\%$  lignin at the surface  
585 to 85% at 143cm. This represents a strong anaerobic preferential degradation of polysaccharides at depth by the microbial community, since no vegetation change has been observed in this core (Blewett, 2021) nor in nearby cores (Wright and Comas, 2016).

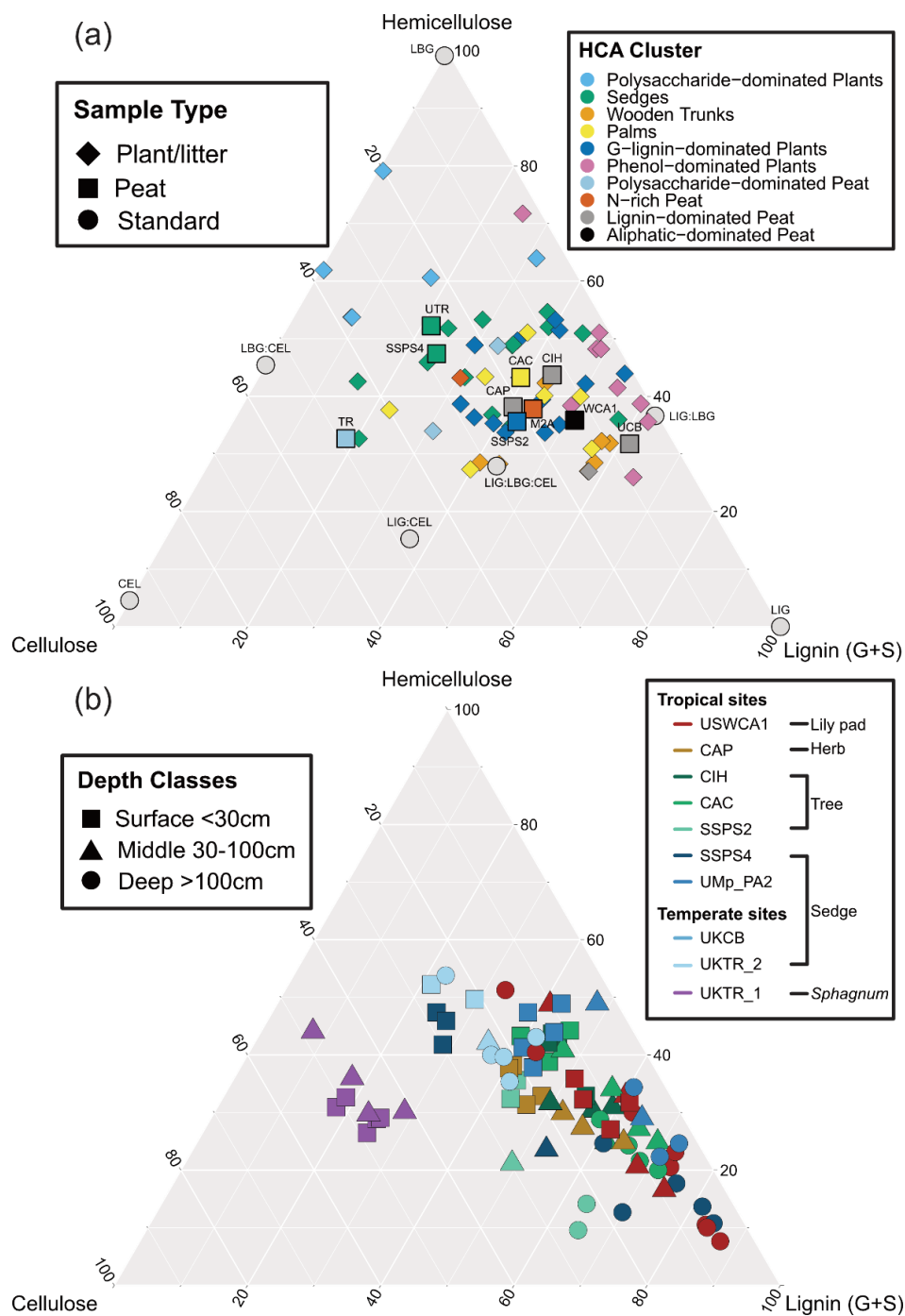


Figure 7: (a) Ternary diagram showing the pyrolytic fingerprint similarity (%) between plant tissues, litters, surface-most peat and analytical standards coloured by their associated HCA cluster. Analytical standards include lignin (LIG), cellulose (CEL) and

590



**hemicellulose (LBG), and 1:1 mixes (e.g. LIG:LBG). (b) Ternary diagram showing the pyrolytic fingerprint similarity (%) between peat depth classes**

595 Pantano is a *Montrichardia*-dominated swamp, which is a common Amazonian ecosystem (Ortiz et al., 2020), but CAP uniquely features a layer of peat. The *Montrichardia* tissues (both leaves and roots) have a lignin-rich macromolecule signature of about 50/50/0%, but this is not reflected in the surface peat, which exhibits the more common 40/40/20% distribution. However, the surface peat already has a distinctive higher proportion of aliphatics, and this feature is apparent in *Montrichardia* leaves. Thus, the surface peat likely has a high contribution of *Montrichardia* leaves and roots as well as  
600 more diverse plant contributions. The % lignin quickly increases in the 70 cm of peat to about 60% at the bottom, exceeding the lignin percentage of any plant material sourced from Pantano, indicating rapid and selective degradation of polysaccharides.

While the plant community in Inirida is yet to be described, the litter samples collected have pyrolysates consistent with a  
605 hardwood origin. S-lignin-rich woody material (Hedges and Mann, 1979), lignin-rich roots and aliphatic-rich leaves (Fig. 7a) are reflected by a high proportion of S-lignin pyrolysates in the peat (Fig. 5). The surface peat has a pyrolysate composition and inferred distribution of plant macromolecules like most of the plants and surface peat (40/40/20% lignin/hemicellulose/cellulose). At shallow depths (> 30 cm), the lignin composition rapidly increases to ~ 60%, which could be a consequence of degradation as inferred for other sites or deposition/persistence of woody tissues. However, a consistent  
610 P/(S+G) ratio (Fig. 8), the lowest in the entire dataset, suggests that the tissues did not significantly change.

Cananguchal is a palm swamp dominated by *Mauritia flexuosa*, a common palm tree in Amazonian peatlands (Winton et al., 2025; Draper et al., 2018). As expected, the upper 40 cm of Cananguchal peat has a pyrolytic fingerprint (40/40/20% lignin/hemicellulose/cellulose) similar to that of the modern palm plants, most likely sustained by the active and dead  
615 pneumatophores present in the peat at this interval. At depths lower than 40 cm the peat shows a distinct aliphatic- and G-lignin-rich profile (Fig. 5), although a high proportion of P-lignin derived from the palm vegetation is maintained throughout the peat profile as shown by the P/(S+G) ratio (Fig. 8). The lignin content increases at depth from 40% to 71% lignin, largely at the expense of hemicellulose components, without changing the proportion of cellulose (~10%) nor the P/(S+G) ratio (Fig. 8). This implies a similar biopolymer preferential degradation.

620 SSPS2 is classified as a mixed palm/hardwood site with *Raphia taedigera* and *Camposperma panamensis* being the dominant vegetation, respectively. All these plant tissues clustered canonically in the HCA analysis, with the surface sample of SSPS2 exhibiting a pyrolytic profile comparable to the leaves from *Camposperma*, and the SSPS2 litter exhibiting a *Raphia* leaf profile (Fig. 5). All plant material, litters and surface peat have a balanced lignin/hemicellulose/cellulose profile  
625 at around 40/40/20%, respectively. At intermediate depths, the proportion of aliphatics and lignin increases, likely reflecting the preservation of *Raphia* root material (Hoyos-Santillan et al., 2015), although all of the vegetation in Panama has a similar



pyrolytic biopolymer profile, clustering together in the HCA. At greater depths, the proportion of lignin increases from 42% to 65%. However, the proportion of cellulose is persistent, unlike nearly all other sites, suggesting better preservation of woody material at depth in SSPS2. In particular, the 178 cm deep sample has a pyrolytic profile similar to the wooden trunks analysed (Fig. 5).

SSPS4 primarily consists of the sawgrass *Cladium mariscus* (Baird et al., 2017; Phillips et al., 1997). This is reflected in the litter and surface peat (up to 17 cm) in SSPS4, both of which have similar pyrolytic profiles to the *Cladium* and other sedges. However, at greater depths the peat becomes dramatically enriched in lignin, typically exceeding 60% and reaching a maximum of 85% lignin. The peat stratigraphy in San San Pond Sak suggests that SSPS4 used to be characterised by an ecosystem similar to SSPS2, indicated by a woody consistency of deep peat in previous studies (Phillips et al., 1997; Swindles et al., 2024). However, the lignin content in deep SSPS4 sites exceeds even the hardwood trunks included in our study (e.g. *Ceiba petandre*, which has %lignin < 57%). Hardwood inputs or selective preservation of hardwood tissues could explain the rapid increase in %lignin between 23 and 58 cm, but further downcore alteration must reflect a continuous enrichment of lignin by selective degradation. For example, the sample from 358 cm has a pyrolytic profile resembling that of wooden trunks (Fig. 5) but still has a 70% lignin signal. Thus, the OM character of deep San San Pond Sak peat is a combination of hardwood input and selective degradation since deposition, collectively representing a transformation of the OM composition since deposition.

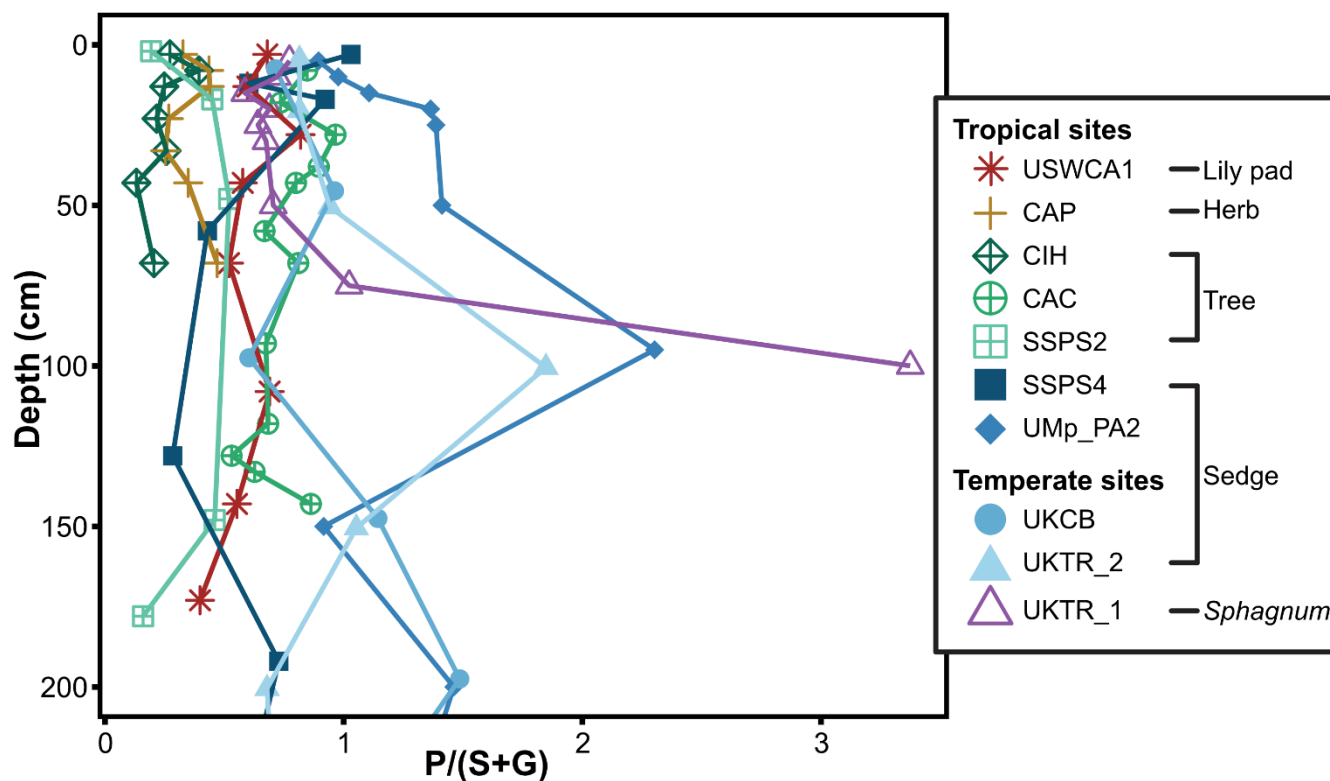
Mpologoma peat pyrolysates are characterized by two clusters in the HCA: a surface cluster that resembles papyrus roots and a deeper aliphatic, phenolic cluster that resembles papyrus leaves. This is evident in their reconstructed plant macromolecular composition, where the surface samples have a 40/40/20% profile similar to most plant material including papyrus roots but contrasting with papyrus leaves which have a more lignin-enriched profile at around 60/20/20%. Furthermore, the P/(S+G) ratio increases at depth (Fig. 8), also indicating a shift in source material from papyrus roots to leaves. Although an increase in leaf relative to root material with depth appears non-intuitive, the top 30 cm might be dominated by active root systems (Kayendeke et al., 2018) that migrate or get recycled by the papyrus plant while dead leaf material in peat horizons is constantly supplied from the surface in greater volumes than dead root material. The deeper Mpologoma cluster is similar to the papyrus leaves but characterized by an even greater, 70%, lignin composition, indicating that both selective preservation and papyrus tissue input govern the composition of the deep Mpologoma peat.

Crymlyn bog is currently a fen dominated by *Phragmites*, which is represented by rather lignin-rich (60%) surface peat (Gadel and Bruchet, 1987). Although Crymlyn Bog has experienced past vegetation change that likely affected its OM composition, it still exhibits evidence for selective enrichment of lignin. Samples from 46, 148, and 198 cm have a profile of 40/50/10%, i.e. a lignin depletion relative to the surface peat. This composition is similar to that of *Sphagnum* plants, and indeed *Sphagnum* was the dominant vegetation at Crymlyn Bog in the past based on both pollen and macrofossil evidence



(Hughes and Dumayne-Peaty, 2002), illustrating how past changes in peat forming vegetation (Schellekens et al., 2012) can overprint downcore degradation processes in some settings. Prior to the *Sphagnum* interval, in deeper peat below 298 cm, *Phragmites* and *Cladium* were Crymlyn bog's dominant vegetation (Hughes and Dumayne-Peaty, 2002). This is reflected by a return to a 60% lignin signature; at even greater depths, 400 and 800 cm, lignin reaches 70%, likely reflecting enhancement  
665 via selective degradation.

Intriguingly, the two cores collected from the Tor Royal bog have considerably different compositions, with the percentage of cellulose at UKTR\_1 being ~ 50% and UKTR\_2 being ~ 20%. This likely reflects the heterogeneity of ombrotrophic bog vegetation, governed by their microtopography (West, 1997). UKTR\_2 was collected on a hummock, currently dominated  
670 by sedges such as cotton grass and exhibiting a characteristic sedge-like pyrolysate profile (Fig. 5), whereas UKTR\_1 was collected in a currently *Sphagnum*-dominated hollow. This is confirmed by the extractable *n*-alkane ratio  $C_{23}/C_{31}$  (Fig. A4), which has values  $> 5$  in UKTR\_1 compared to  $< 5$  in UKTR\_2, reflecting a higher *Sphagnum* contribution in the former (Nott et al., 2000). These differences are also reflected in a higher proportion of cellulose-derived pyrolysates in the latter site (Fig. 7b). The UKTR\_1 surface peat has a unique macromolecular composition that is more polysaccharide-rich than any of our  
675 other sites (20/30/50% lignin/hemicellulose/cellulose), while UKTR\_2 is also polysaccharide-rich (20/50/30% lignin/hemicellulose/cellulose) but has a distribution that is consistent with sedges being the primary OM constituent. At depth (20 to 100 cm), UKTR\_1 peat exhibits a decrease in %lignin, suggesting that *Sphagnum* dominance is greater during this interval, perhaps at the expense of cotton grass roots that were observed at the site and in the shallow core. In UKTR\_2 the proportion of lignin increases but only to ~ 40%, even at 5 meter deep. This could reflect the very low lignin contents of  
680 the peat-forming vegetation, which imposes constraints on downcore lignin-enrichment. However, this contrasts remarkably with the other sites in this study, suggesting minimal degradation. This is consistent with previous reports for *Sphagnum* and its inherent anti-microbial properties that slow degradation, especially in deeper anoxic horizons (Abbott et al., 2013; Van Der Heijden et al., 1997).



685

**Figure 8: Downcore plot of the P/(S+G) ratio, where P = phenols, G = guaiacols, and S = syringols, in all our sites.**

While most sites have depositional tissue/vegetation histories that complicate their OM composition and downcore profiles, nearly all of them exhibit an enrichment of lignin at depth. The preferential degradation of polysaccharides appears to persist across all depths, i.e. continuing to decrease even in the catotelm, indicating that these fresh plant biopolymers are used as substrate for microbial growth regardless of the complexity and limitations of depolymerization of biopolymers under anoxia (Mcgovern et al., 2021; Freeman et al., 2001). Although this general trend has been previously reported (Ryan et al., 1987; Schellekens et al., 2012; Upton et al., 2018), our work reveals the more severe and consistent transformation of peat OM in the tropics compared to the temperate sites. This occurs despite high starting lignin contents associated with lignin-rich plants and tissues, such that deep tropical peat becomes profoundly enriched in lignin (and aliphatics) even at relatively shallow depths (< 50 cm in some cases).

690

Furthermore, our data reveal the variety of OM compositions of peat forming plants and especially the impact of the presence of some plant tissues with particularly high lignin contents and inferred recalcitrance, such as a high proportion of lignin in wooden trunks, Papyrus leaves, and *Montrichardia* leaves. These tissues are preferentially preserved and govern the downcore changes in peat OM, contributing to enrichment of lignin at depth; in the case of woody tissues, this also facilitates

700



the preservation of cellulose at depth (Van Der Heijden and Boon, 1994). This complements previous work showing the slow degradation of *Sphagnum* dominated peat (Van Der Heijden et al., 1997).

705 Due to these multiple factors, lignin proportions can reach ~ 85% in deep tropical peat, which is approximately twice that of  
the starting material. Given the overall recalcitrance of lignin to degradation, especially under anaerobic conditions (Freeman  
et al., 2001; Freeman et al., 2004), this suggests that deep peat is a poor substrate for microbial growth. However, peat never  
fully depletes of polysaccharides, and even in the most degraded peat, hemicelluloses persist at depth. These hemicelluloses  
are likely covalently bonded or entrenched in the lignocellulosic complex and protected by the aromatic and ether bonds  
710 (Melillo et al., 1989) and slower anaerobic experiments (Hoyos-Santillan et al., 2015).

These results have implications for the reactivity of deep tropical peat OM, which apparently remains a viable substrate for  
microbial growth despite high aromatic contents (Pavia et al., 2024; Girkin et al., 2020), as well as the fate of that OM under  
anthropogenic climate change and/or re-exposure to oxidising conditions (Könönen et al., 2016).

715

### 3.3.2 The OM lability decreases logarithmically with depth consistently across lowland tropical peatlands

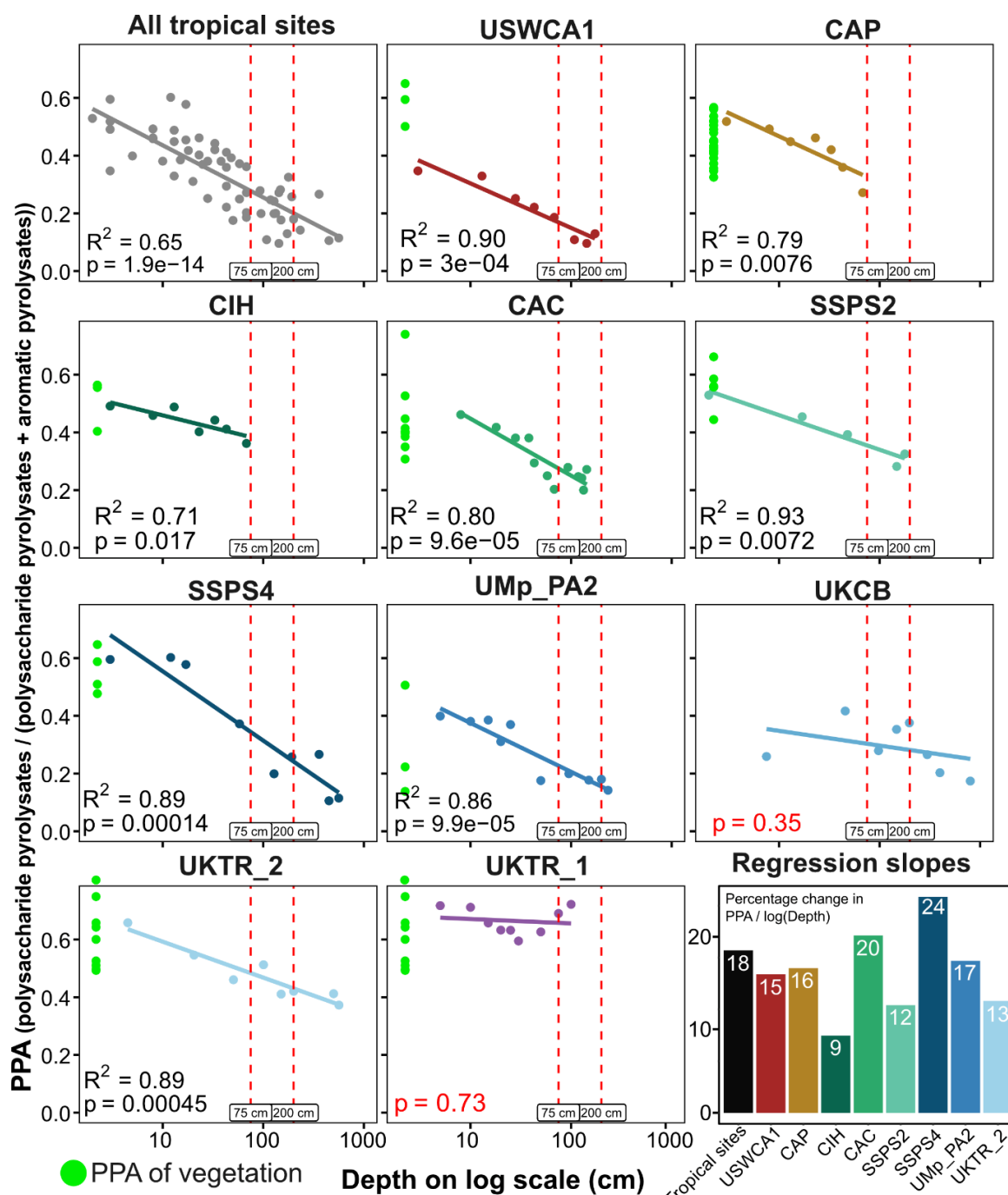
Multiple factors govern the reactivity of OM, but lignin is generally considered to be less reactive and more recalcitrant than  
polysaccharides (Gunina and Kuzyakov, 2022). This is especially true under anoxic conditions (Freeman et al., 2001;  
Freeman et al., 2004), although the simplistic interpretation of polysaccharide macromolecules as labile can be complicated  
720 by their associations with lignin in plant tissues (Dumitrache et al., 2017). Similarly, condensed and polymerised (i.e.  
humified) OM, as partly represented by the aliphatic/aromatic enrichment of peat, is generally considered to be less reactive  
than biomacromolecules (Gunina and Kuzyakov, 2022). Regardless of chemical composition, OM must become more  
recalcitrant with burial depth due to the selective degradation of more labile components. Consequently, it appears that  
tropical peats from greater than 50 cm depth are particularly recalcitrant to microbial degradation.

725

Given that recalcitrance is an emergent property of both selective preservation and humification, i.e. resistant biomolecules  
and geomolecules, we employ a more chemically agnostic ratio for assessing site-specific downcore differences in OM  
composition: the PPA ratio (polysaccharide pyrolysates / (polysaccharide pyrolysates + aromatic pyrolysates)). It is similar  
in scope to the FTIR-based ratios (Upton et al., 2018; Artz et al., 2006), <sup>13</sup>C-NMR-based ratios (Normand et al., 2021) and  
730 the lignocellulose index (LCI) based on wet chemistry separation (Inglett et al., 2012; Melillo et al., 1989) but it has some  
microbiological justification, particularly at anoxic depths. The enzyme “latch” theory argues that the breakdown of aromatic  
bonds is limited under anoxic conditions due to the dominance of oxygen-dependent phenol oxidases as the primary  
enzymes in their degradation (Freeman et al., 2001; Freeman et al., 2004). Therefore, the pyrolysates associated with



735 polysaccharides represent the macromolecular “labile” material, being energetically more available and having diverse and largely uninhibited metabolic potential under anoxia (Gunina and Kuzyakov, 2022; Mcgovern et al., 2021).





740 **Figure 9: Individual cross plots per site and all tropical sites showing the PPA against the logarithm of depth (log(cm)). Trendlines represent the linear regression (Pearson) per plot with  $R^2$  and p-values included. The regression slopes are shown in the bottom right corner and for all sites a significant correlation was observed. Red dashed lines represent 75 cm and 200 cm depth aiding depth intuition in the logarithmic space.**

In our dataset, the PPA ratio decreases with depth across most peat profiles (Fig. 2a), like the downcore decrease in cellulose and hemicellulose relative to lignin we described (Fig. 7a). Despite the major compositional differences among the diverse plant communities in each site (PPA = 0.65–0.35), the downcore changes in PPA ratios are remarkably consistent. Most notably, the PPA ratio shows a logarithmic decrease with depth with high significance and a strong fit at every site except UKTR\_1 and UKCB (Fig. 9). This logarithmic relationship is particularly strong in the tropical sites and appears to persist at depth, with aromatic proportions continuing to increase below 100 cm depth (Fig. 9). The slopes of the natural logarithmic fit, %decrease PPA / log(cm), range from 9 to 24%, suggesting a similar magnitude of preferential degradation across all sites (Fig. 9). However, the basement ages of our lowland tropical peat span from decades to millennia producing accumulation rates that span three orders of magnitudes and which are higher than the accumulation rates in the temperate peatlands (Table S5). This suggests that preferential degradation exhibits large differences in the time domain with much higher preferential degradation rates in the tropics compared to temperate peats, likely due to the higher temperatures in the tropics. Furthermore, although SSPS4 and UKTR\_2 have similar PPA at the surface (0.65), UKTR\_2 exhibits a much slower preferential degradation profile. The slower degradation at UKTR\_2, combined with the lack of clear correlation between depth and PPA at UKCB and UKTR\_1 ( $p > 0.05$ ), further indicates that the preferential degradation of polysaccharides relative to aromatic macromolecules is slower in temperate peatlands than at tropical sites. At these temperate sites, either slow rates of degradation are observed or downcore degradation is obscured by historic vegetation changes (Uhelski et al., 2022). Consequently, Schellekens et al. (2009) and others have been able to utilise pyrolysate abundance of lignin and polysaccharides as vegetation as well as decomposition markers. The wider use of py-GC-MS for vegetation reconstruction in the temperate peatland literature (Schellekens et al., 2015; Schellekens et al., 2009; Mcclymont et al., 2011; Carr et al., 2010) suggests that the strong correlation between depth and the PPA ratio is primarily a lowland tropical feature (Fig. 9).

This has consequences for biogeochemical processes in deep peat, including greenhouse gas emissions. Peats with lower PPA ratios are characterised by higher anaerobic  $\text{CO}_2:\text{CH}_4$  production ratios at higher temperatures (Inglett et al., 2012; Sihi et al., 2016), which suggests the importance of reactive substrates for methanogenesis, although lignin cannot be discounted as a substrate for methanogenesis (Liu et al., 2025). Our data show that the pronounced downcore shift to a more aromatic composition seen across our tropical sites could drive the higher  $\text{CO}_2$  than  $\text{CH}_4$  emissions observed across tropical peatland systems (Wright et al., 2011), further highlighting the control OM quality has on carbon cycle dynamics.



### 3.3.3 Interactions of the peat macromolecular composition and the microbial community; degradation and home-field advantage

770

The downcore changes in peat OM composition also have implications for deep peat biogeochemistry and microbiology. Plant biopolymers depolymerize during the first steps of OM degradation, often through fungi using oxygen-dependent, macromolecule-modifying enzymes (Yarwood, 2018). These obligate aerobic fungi are suppressed under anaerobic wetland conditions and mostly act on standing biomass or recent plant litter (Yarwood, 2018; Wang et al., 2021). Although fungi generally degrade lignin and cellulose more quickly than bacteria (Thormann, 2006), bacterial lignin modifying enzymes and cellulases are common in peatlands (Burns et al., 2013). Extracellular lignin modifying enzymes are widespread among prokaryotes (Janusz et al., 2017; Janusz et al., 2020) and a wide array of bacteria has cellulose degradation potential including Chloroflexi, Bacteroidetes, Gemmatimonadetes, and Planctomycetes (Baker et al., 2015). These bacteria thrive under aerobic conditions and are responsible for depolymerization in the oxic horizon (Yarwood, 2018). After the depolymerization of lignocellulose, subsequent degradation of released monomers and dimers can be mediated by a more diverse microbial community (Juottonen et al., 2017).

775

780

Small molecules derived from aerobic biopolymer degradation can be readily utilised under anaerobic conditions, but the continued degradation of plant biopolymers under anaerobic conditions becomes enzymatically challenging (Mcgovern et al., 2021). For example, under anaerobic conditions, the proposed ‘enzymic latch’ (Freeman et al., 2001) could inhibit the further degradation of lignocellulose. Furthermore, polyphenols are toxic to microorganisms, can inactivate enzymes and bind substrates, so their accumulation can also inhibit saccharide degradation (Fenner and Freeman, 2020). However, other studies (Urbanova and Hajek, 2021; Mcgovern et al., 2021) found that polyphenol degradation products could be generated under anaerobic conditions, showing metabolite and enzyme signatures, as well as uninhibited degradation of polysaccharides. Moreover, lignin can be utilized by some members of the Bathyarchaeia anaerobically through O-demethylation of lignin monomers, although enzymes of anaerobic depolymerisation remain elusive (Yu et al., 2022). O-demethylation reduces the methoxy-groups of lignin monomers to hydroxyl moieties, using them as an energy and carbon source (Yu et al., 2018; Hou et al., 2023).

785

790

795

800

Aside from the role of redox state, lignin is more recalcitrant to degradation than cellulose because of the higher energy investment due to its chemical complexity (Gunina and Kuzyakov, 2022), as reflected by the diversity of lignin-modifying-enzymes (Janusz et al., 2017). Differences in degradation rates can be mitigated via enhanced extracellular lignase and cellulase activity under higher temperatures, due to higher kinetic efficiency of the associated enzymes (Chen et al., 2020). However, this contrasts with our finding of pronounced aromatic enrichment in the tropical sites. Given increasing evidence for abundant Bathyarchaeia in deep peat (Pavia et al., 2024) and their lignin-degrading capacity (Dong et al., 2025; Yu et al., 2018), we do not suggest that lignin degradation has ceased. However, aromatic enrichment at depth indicates the continued and more rapid degradation of other biopolymers. The deep peat microbial community includes a wide variety of Archaea



and Bacteria with polysaccharide-degrading capacities (Pavia, 2024). In fact, even the aforementioned Bathyarchaea are metabolically diverse, likely contributing to multiple downstream OM degradation pathways in deep peat (Pavia et al., 805 2024).

Collectively, our data and previous work suggest that differential degradation of biopolymers is enhanced at tropical sites and occurs under both oxic and anoxic conditions, resulting in a progressive increase in tropical peat aromaticity. Moreover, the logarithmic decrease in polysaccharide content suggests that OM becomes increasingly recalcitrant at depth. A decrease 810 in peat OM reactivity with depth was also observed by Hoyos-Santillan et al. (2015), who attributed this to low oxygen or enzyme penetration in the peat profile. Our work suggests that the increasingly refractory character of the OM is also an important control on the rates of peat degradation. This contributes to our understanding of why depth is such an important variable in microbial diversity in tropical peatlands (Too et al., 2018; Dom et al., 2021) and general wetland microbiome functioning (Borton et al., 2025).

815

Future work should explore other factors governing peat reactivity. Given the variability in peat-forming vegetation and its susceptibility to environmental change (Page et al., 2022), we suggest that the so-called homefield-advantage (HFA) could also be important. HFA theory argues for an intimate interaction between the microbial community and OM composition (see Dehaen et al., 2025 and references therein), such that subtle differences in OM character cause specialisation in the 820 microbial community and their capacity to degrade that specific peat substrate (Austin et al., 2014). Previous studies have shown that allochthonous leaf litter introduced to peat decomposes more slowly than autochthonous leaf litter, suggesting that the peat microbial community is moulded to the latter (Hoyos-Santillan et al., 2017). Our HCA analysis detects in even highly degraded peat a macromolecular fingerprint of the vegetation from which that peat formed. This confirms a macromolecular basis for HFA; in fact, HFA could persist even in deep (> 50 cm) peat, reflecting the molecular composition 825 of ancient peat-forming vegetation communities. Taken together, there are likely multiple interactions between the microbial community function and the macromolecular composition of peat. The microbial community is optimized to degrade the litter from its specific peatland vegetation, from the most labile material at the top of the profile to the most recalcitrant “leftovers” at the basement.

#### 4 Conclusion

830 In this work, we explored the OM characteristics of a range of tropical and two temperate peatlands. We demonstrated the applicability and utility of py-GC-MS to gain insight into the peat macromolecular composition of lowland tropical peatlands in comparison to FTIR, which featured limits, likely due to silicate mineral interference in some of the tropical sites. We characterized major trends in our dataset of downcore peat profiles and vegetation, such as a strong decomposition signal as indicated by an enrichment of aromatic and aliphatic macromolecules. We also show that the source vegetation showed



- 835 unique pyrolytic signatures, which could still be detected in the peat that had undergone intense degradation and at depth (> 50 cm). These pyrolytic signatures imply a unique vegetation signal retained in the peat that could form a chemical basis to the home advantage theory. Furthermore, selective degradation of polysaccharides to aromatic biopolymers follows a natural logarithmic decline with depth and the slope is consistent across all sites. This indicates that lowland tropical peatlands have a uniform decomposition regime, which leaves the peat OM highly aromatic (and aliphatic) in character in deeper horizons.
- 840 The aromaticity of peat at depth can help explain why depth is such an important variable in microbial diversity in tropical peatlands, which aids our understanding of how peat will respond to human-induced degradation and global warming on the global scale of tropical peatlands. Furthermore, this study can serve as a basis for integrating OM pools into tropical peat accumulation models, furthering our understanding of tropical peat dynamics.



## Appendix A

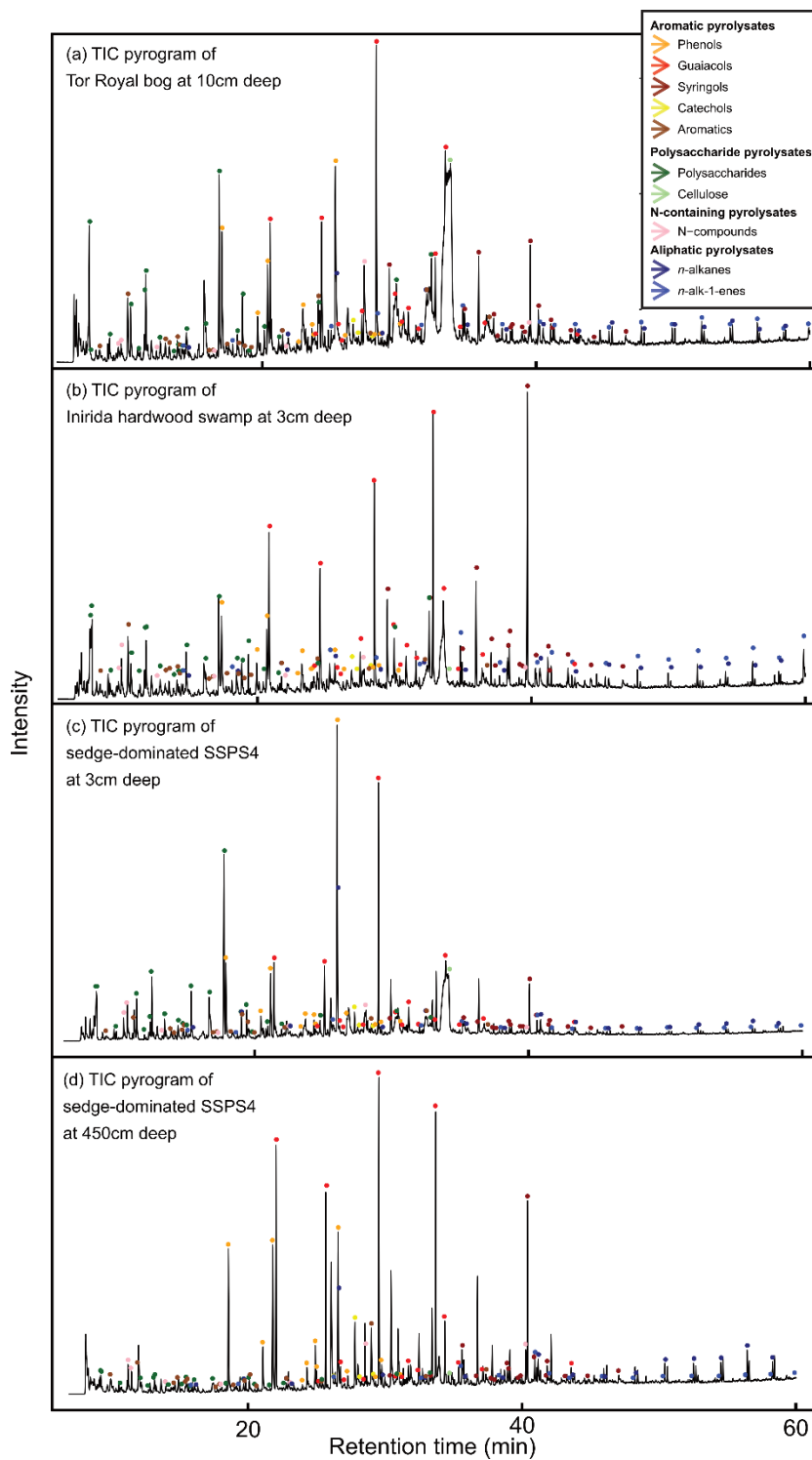




**Figure A1: Pyrograms of three surface samples with different vegetation covers and a deep sample. (a) Surface sample at TR shows plenty of polysaccharides which are enriched in Sphagnum material. (b) CIH shows high peak of syringols which are abundant in hardwood. (c) Surface sample of SSPS4 shows a large peak of P3 (Vinyl-phenol) which is a sedge biomarker. (d) The deep sample of SSPS4 is marked by lacking polysaccharide peaks by extended degradation.**

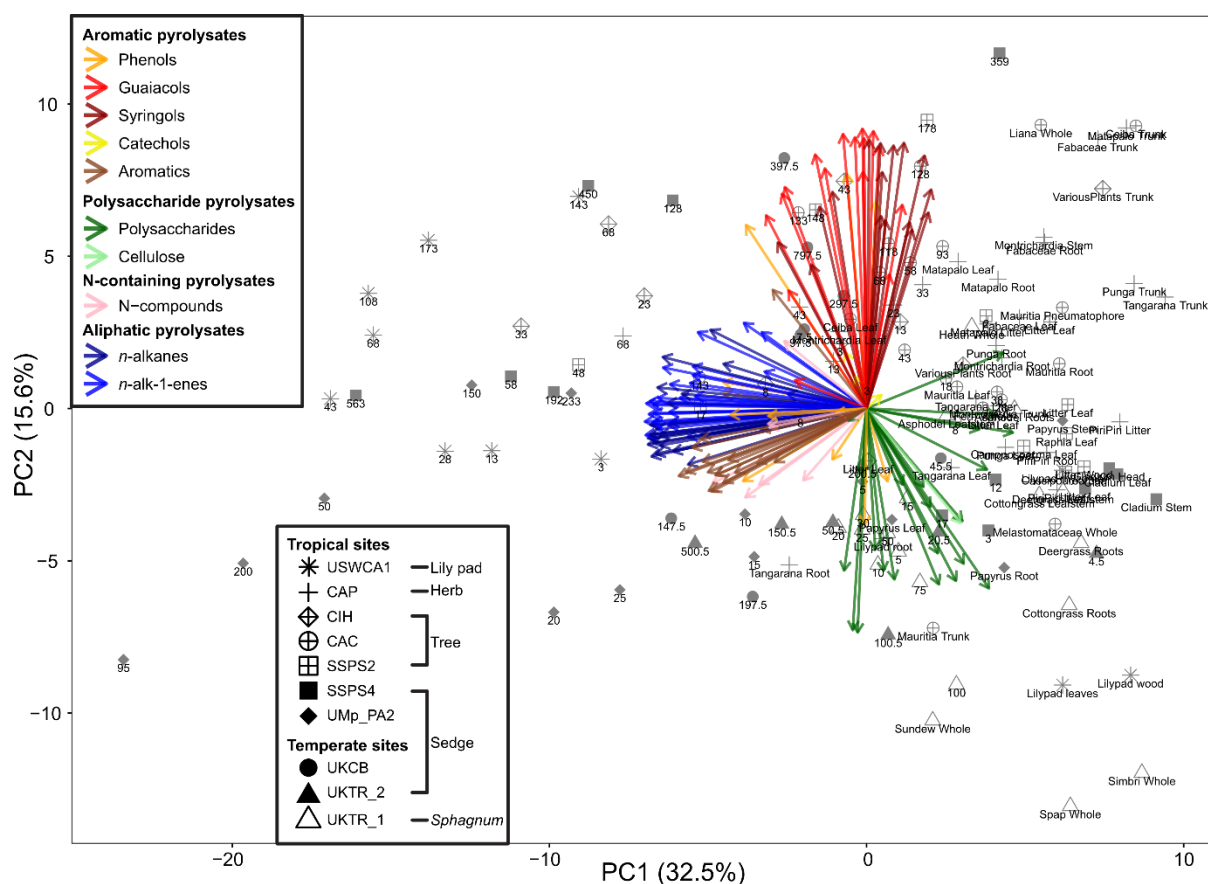
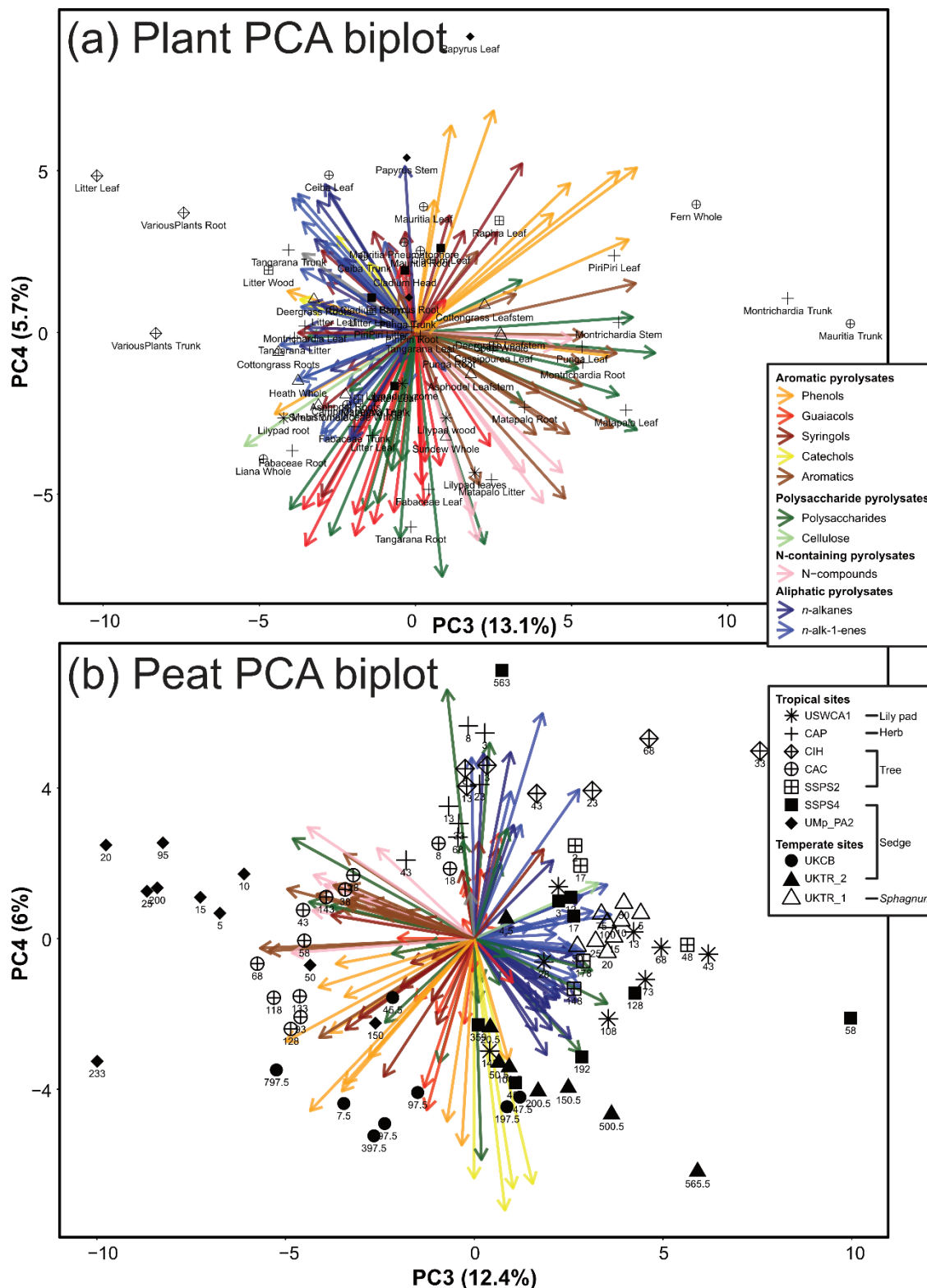


**Figure A2: PCA biplot on the normalized pyrolysate fractional abundances of the peat and plant dataset combined. Vectors are individual pyrolysates coloured on their canonical macromolecular assignment.**

850





855 **Figure A3: PCA biplot of PC3 and PC4 on the normalized pyrolysate fractional abundances in the A) plant and B) peat dataset separately. Vectors are individual pyrolysates coloured on their canonical macromolecular assignment.**

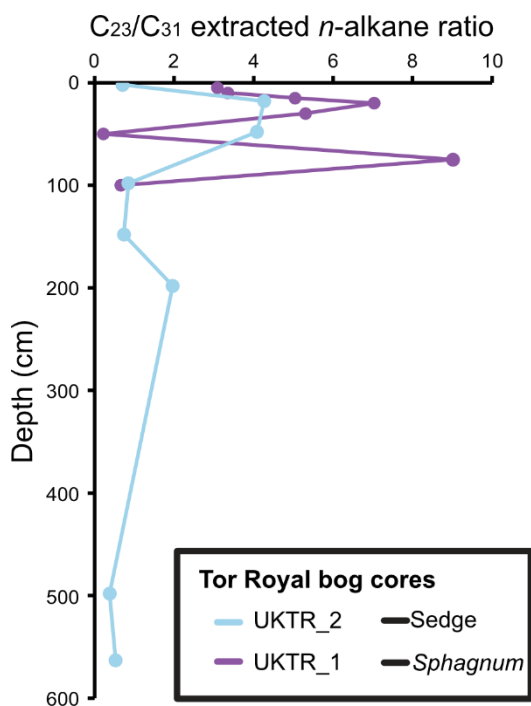


**Figure A4: Extractable n-alkane ratio  $C_{23}/C_{31}$  which represents Sphagnum contribution in UKTR\_2 and UKTR\_1. UKTR\_1 shows a higher abundance of Sphagnum, collected in a hollow, while UKTR\_2 has less Sphagnum, collected in a hummock.**

#### Data availability

860 The supplementary tables will be made publicly available through OSF (Open Science Foundation)

<https://doi.org/10.17605/OSF.IO/YZWT7>

#### Author contributions

MV, RDP, and JB conceptualized the study; fieldwork was supported by MV, MNJ, YZ, AO, SMKC, PP, SR, JB, PAP, JCB, DAA, FK, EJK, CK, and AVGS; methodology was developed by MV and RHP; lab work was conducted by MV, MNJ, SM, RHP, YZ, TAH, PP, and SR; project was administered and supervised by RDP, BDAN, CB, and AVGS; 865 visualisation was completed by MV; original draft was written by MV; reviewing and editing was conducted by MV, MNJ, SM, RHP, YZ, TAH, AO, SMKC, PP, SR, JB, PAP, DAA, FK, EJK, CK, CK, BDAN, CB, AVGS, and RDP



### Competing interests

The authors declare that they have no conflict of interest.

### 870 Disclaimer

Copernicus Publications remains neutral with regard to jurisdictional claims made in the text, published maps, institutional affiliations, or any other geographical representation in this paper. While Copernicus Publications makes every effort to include appropriate place names, the final responsibility lies with the authors. Views expressed in the text are those of the authors and do not necessarily reflect the views of the publisher.

### 875 Acknowledgements

First, we acknowledge the people safekeeping and managing these incredible peatlands included in this study such as the Ticuna, Micosukee, Seminole, Caño Vitina, PNN Amacayacu, Smithsonian Tropical Research Institute, Wetlands Management Department, and Natural England. We further thank the technical support of Odu Okoturo-Evans and Duncan Atkinson in the School of Chemistry at the University of Bristol for the FTIR analyses and the technical support of Fotis Sgouridis in the School of Geography at the University of Bristol for the EA analyses.

### Financial support

M. Vreeken is funded through PhD studentships at the Great Western Alliance Doctoral Training Partnership (NERC GW4+ DTP2) [NE/S007504/1]. R.D. Pancost, C. Bryce, A.V. Gallego-Sala, B.D.A. Naafs, R.H. Peel, A. Oakeshott, T.A. Halamka, S.M.K. Cheung, and P. Prokopiou acknowledge funding from UK Research and Innovation (UKRI) under the UK government's Horizon Europe funding guarantee [CERES EP/X023214/1] and R.D. Pancost, C. Bryce, A.V. Gallego-Sala, B.D.A. Naafs, M.N. Jenkins, and Y. Zhang acknowledge funding from the Leverhulme Trust [BACC RPG-2022-245]. Juan C. Benavides and D.P. Alarcon Prado acknowledge funding by the National Academies of Sciences, Engineering, and Medicine under the PEER program (grant code 9-166). B.D.A. Naafs also acknowledges funding through a Royal Society Tata University Research Fellowship. A.V. Gallego-Sala acknowledges funding from the European Research Council (ERC) under the European Union's Horizon 2020 research and innovation programme (grant agreement no. 865403). The authors also wish to thank the NERC for partial funding of the National Environmental Isotope Facility (NEIF; contract no. NE/V003917/1).



## Review statement

## References

- 895 Abbott, G. D., Swain, E. Y., Muhammad, A. B., Allton, K., Belyea, L. R., Laing, C. G., and Cowie, G. L.: Effect of water-table fluctuations on the degradation of Sphagnum phenols in surficial peats, *Geochimica et Cosmochimica Acta*, 106, 177–191, <https://doi.org/10.1016/j.gca.2012.12.013>, 2013.
- Abiy, A. Z., Melesse, A. M., Abteu, W., and Whitman, D.: Rainfall trend and variability in Southeast Florida: Implications for freshwater availability in the Everglades, *PLoS One*, 14, e0212008, <https://doi.org/10.1371/journal.pone.0212008>, 2019.
- 900 Abteu, W., Obeysekera, J., and Iricanin, N.: Pan evaporation and potential evapotranspiration trends in South Florida, *Hydrological Processes*, 25, 958–969, <https://doi.org/10.1002/hyp.7887>, 2011.
- Alcaniz, J., Romera, J., Comellas, L., Munne, R., and Puigbo, A.: Effects of some mineral matrices on flash pyrolysis-GC of soil humic substances, *Science of The Total Environment*, 81–82, 81–90, [https://doi.org/10.1016/0048-9697\(89\)90113-7](https://doi.org/10.1016/0048-9697(89)90113-7), 1989.
- 905 Amesbury, M. J., Charman, D. J., Fyfe, R. M., Langdon, P. G., and West, S.: Bronze Age upland settlement decline in southwest England: testing the climate change hypothesis, *Journal of Archaeological Science*, 35, 87–98, <https://doi.org/10.1016/j.jas.2007.02.010>, 2008.
- Artz, R., Chapman, S., and Campbell, C.: Substrate utilisation profiles of microbial communities in peat are depth dependent and correlate with whole soil FTIR profiles, *Soil Biology and Biochemistry*, 38, 2958–2962, <https://doi.org/10.1016/j.soilbio.2006.04.017>, 2006.
- 910 Austin, A. T., Vivanco, L., Gonzalez-Arzac, A., and Perez, L. I.: There's no place like home? An exploration of the mechanisms behind plant litter-decomposer affinity in terrestrial ecosystems, *New Phytologist*, <https://doi.org/10.1111/nph.12959>, 2014.
- Baird, A. J., Low, R., Young, D., Swindles, G. T., Lopez, O. R., and Page, S.: High permeability explains the vulnerability of the carbon store in drained tropical peatlands, *Geophysical Research Letters*, 44, 1333–1339, <https://doi.org/10.1002/2016gl072245>, 2017.
- Baker, B. J., Lazar, C. S., Teske, A. P., and Dick, G. J.: Genomic resolution of linkages in carbon, nitrogen, and sulfur cycling among widespread estuary sediment bacteria, *Microbiome*, 3, 14, <https://doi.org/10.1186/s40168-015-0077-6>, 2015.
- Blewett, J.: Determining the factors shaping archaeal communities and methane production pathways in tropical wetlands: a lipid biomarker, stable carbon isotopic and 16S rRNA gene approach, School of Chemistry, University of Bristol, Bristol, 2021.
- 920 Blewett, J., Naafs, B. D. A., Gallego-Sala, A. V., and Pancost, R. D.: Effects of temperature and pH on archaeal membrane lipid distributions in freshwater wetlands, *Organic Geochemistry*, 148, <https://doi.org/10.1016/j.orggeochem.2020.104080>, 2020.
- 925 Boom, A., Sinnige Damsté, J. S., and de Leeuw, J. W.: Cutan, a common aliphatic biopolymer in cuticles of drought-adapted plants, *Organic Geochemistry*, 36, 595–601, <https://doi.org/10.1016/j.orggeochem.2004.10.017>, 2005.



- Boon, J. J., Dupont, L., and De Leeuw, J. W.: Characterization of a peat bog profile by Curie point pyrolysis-mass spectrometry combined with multivariant analysis and by pyrolysis gas chromatography-mass spectrometry, *Peat and Water*, 215–239, 1986.
- 930 Borton, M. A., Oliverio, A. M., Narrowe, A. B., Villa, J. A., Rinke, C., Hoyt, D. W., Liu, P., McGivern, B. B., Bechtold, E. K., Ellenbogen, J. B., Daly, R. A., Smith, G. J., Angle, J. C., Flynn, R. M., Freiburger, A. P., Louie, K. B., Stemple, B., Northen, T. R., Henry, C., Miller, C. S., Morin, T. H., Bohrer, G., and Wrighton, K. C.: Mapping the soil microbiome functions shaping wetland methane emissions, *BioRxiv*, <https://doi.org/10.1101/2024.02.06.579222>, 2025.
- 935 Bunyangha, J., Majaliwa, M. J. G., Muthumbi, A. W., Gichuki, N. N., and Egeru, A.: Past and future land use/land cover changes from multi-temporal Landsat imagery in Mpologoma catchment, eastern Uganda, *The Egyptian Journal of Remote Sensing and Space Science*, 24, 675–685, <https://doi.org/10.1016/j.ejrs.2021.02.003>, 2021.
- Burns, R. G., DeForest, J. L., Marxsen, J., Sinsabaugh, R. L., Stromberger, M. E., Wallenstein, M. D., Weintraub, M. N., and Zoppini, A.: Soil enzymes in a changing environment: Current knowledge and future directions, *Soil Biology and Biochemistry*, 58, 216–234, <https://doi.org/10.1016/j.soilbio.2012.11.009>, 2013.
- 940 Burt, T. P. and Holden, J.: Changing temperature and rainfall gradients in the British Uplands, *Climate Research*, 45, 57–70, <https://doi.org/10.3354/cr00910>, 2010.
- Buurman, P., Nierop, K. G. J., Pontevedra-Pombal, X., and Martínez Cortizas, A.: Chapter 10 Molecular chemistry by pyrolysis–GC/MS of selected samples of the Penido Vello peat deposit, Galicia, NW Spain, in: *Peatlands - Evolution and Records of Environmental and Climate Changes, Developments in Earth Surface Processes*, 217–240, 10.1016/S0928-945 2025(06)09010-9, 2006.
- Carr, A. S., Boom, A., Chase, B. M., Roberts, D. L., and Roberts, Z. E.: Molecular fingerprinting of wetland organic matter using pyrolysis-GC/MS: an example from the southern Cape coastline of South Africa, *Journal of Paleolimnology*, 44, 947–961, <https://doi.org/10.1007/s10933-010-9466-9>, 2010.
- 950 Chadburn, S. E., Burke, E. J., Gallego-Sala, A. V., Smith, N. D., Bret-Harte, M. S., Charman, D. J., Drewer, J., Edgar, C. W., Euskirchen, E. S., Fortuniak, K., Gao, Y., Nakhavali, M., Pawlak, W., Schuur, E. A. G., and Westermann, S.: A new approach to simulate peat accumulation, degradation and stability in a global land surface scheme (JULES vn5.8\_accumulate\_soil) for northern and temperate peatlands, *Geoscientific Model Development*, 15, 1633–1657, <https://doi.org/10.5194/gmd-15-1633-2022>, 2022.
- 955 Chambers, F. M., Beilman, D. W., and Yu, Z.: Methods for determining peat humification and for quantifying peat bulk density, organic matter and carbon content for palaeostudies of climate and peatland carbon dynamics, *Mires and Peat*, 7, 1–10, <https://doi.org/https://doi.org/10.19189/001c.128415>, 2011.
- Charman, D. J., Aravena, R., Bryant, C. L., and Harkness, D. D.: Carbon isotopes in peat, DOC, CO<sub>2</sub>, and CH<sub>4</sub> in a Holocene peatland on Dartmoor, southwest England, *Geology*, 27, 539–542, [https://doi.org/10.1130/0091-7613\(1999\)027<0539:CIIPDC>2.3.CO;2](https://doi.org/10.1130/0091-7613(1999)027<0539:CIIPDC>2.3.CO;2), 1999.
- 960 Chen, J., Elsgaard, L., van Groenigen, K. J., Olesen, J. E., Liang, Z., Jiang, Y., Laerke, P. E., Zhang, Y., Luo, Y., Hungate, B. A., Sinsabaugh, R. L., and Jorgensen, U.: Soil carbon loss with warming: New evidence from carbon-degrading enzymes, *Global Change Biology*, 26, 1944–1952, <https://doi.org/10.1111/gcb.14986>, 2020.
- Chimner, R. A. and Ewel, K. C.: A Tropical Freshwater Wetland: II. Production, Decomposition, and Peat Formation, *Wetlands Ecology and Management*, 13, 671–684, <https://doi.org/10.1007/s11273-005-0965-9>, 2005.



- 965 Chombo, O., Lwasa, S., and Makooma, T. M.: Spatial differentiation of small holder farmers' vulnerability to climate change in the Kyoga plains of Uganda, *American Journal of Climate Change*, 7, 624–648, 2018.
- Cole, L. E. S., Åkesson, C. M., Hapsari, K. A., Hawthorne, D., Roucoux, K. H., Girkin, N. T., Cooper, H. V., Ledger, M. J., O'Reilly, P., and Thornton, S. A.: Tropical peatlands in the anthropocene: Lessons from the past, *Anthropocene*, 37, <https://doi.org/10.1016/j.ancene.2022.100324>, 2022.
- 970 Dehaen, E. M., Burke, E. J., Chadburn, S. E., Kaduk, J., Sitch, S., Smith, N. D., and Gallego-Sala, A. V.: Drivers of soil heterotrophic respiration in tropical peatlands: a review to inform peat carbon accumulation modelling, *Frontiers in Geochemistry*, 3, <https://doi.org/10.3389/fgeoc.2025.1492386>, 2025.
- Deshmukh, A. P., Simpson, A. J., Hadad, C. M., and Hatcher, P. G.: Insights into the structure of cutin and cutan from *Agave americana* leaf cuticle using HRMAS NMR spectroscopy, *Organic Geochemistry*, 36, 1072–1085, 975 <https://doi.org/10.1016/j.orggeochem.2005.02.005>, 2005.
- Dom, S. P., Ikenaga, M., Lau, S. Y. L., Radu, S., Midot, F., Yap, M. L., Chin, M. Y., Lo, M. L., Jee, M. S., Maie, N., and Melling, L.: Linking prokaryotic community composition to carbon biogeochemical cycling across a tropical peat dome in Sarawak, Malaysia, *Scientific Reports*, 11, 6416, <https://doi.org/10.1038/s41598-021-81865-6>, 2021.
- 980 Dong, L., Jing, Y., Hou, J., Zhou, J., Yu, T., Chen, S., Liang, L., Zhu, P., Zhao, X., Hinrichs, K. U., and Wang, F.: A dominant subgroup of marine Bathyarchaeia assimilates organic and inorganic carbon into unconventional membrane lipids, *Nature Microbiology*, 10, 2579–2590, <https://doi.org/10.1038/s41564-025-02121-5>, 2025.
- Draper, F. C., Honorio Coronado, E. N., Roucoux, K. H., Lawson, I. T., A. Pitman, N. C., A. Fine, P. V., Phillips, O. L., Torres Montenegro, L. A., Valderrama Sandoval, E., Mesones, I., García-Villacorta, R., Arévalo, F. R. R., and Baker, T. R.: Peatland forests are the least diverse tree communities documented in Amazonia, but contribute to high regional beta-diversity, *Ecography*, 41, 1256–1269, <https://doi.org/10.1111/ecog.03126>, 2018.
- 985 Dumitrache, A., Tolbert, A., Natzke, J., Brown, S. D., Davison, B. H., and Ragauskas, A. J.: Cellulose and lignin colocalization at the plant cell wall surface limits microbial hydrolysis of *Populus* biomass, *Green Chemistry*, 19, 2275–2285, <https://doi.org/10.1039/c7gc00346c>, 2017.
- Eglinton, G. and Hamilton, R. J.: Leaf Epicuticular Waxes: The waxy outer surfaces of most plants display a wide diversity of fine structure and chemical constituents, *Science*, 156, 1322–1335, <https://doi.org/10.1126/science.156.3780.1322>, 1968.
- 990 Fenner, N. and Freeman, C.: Woody litter protects peat carbon stocks during drought, *Nature Climate Change*, 10, 363–369, <https://doi.org/10.1038/s41558-020-0727-y>, 2020.
- Freeman, C., Ostle, N., and Kang, H.: An enzymic 'latch' on a global carbon store, *Nature*, 409, 149, <https://doi.org/10.1038/35051650>, 2001.
- 995 Freeman, C., Ostle, N. J., Fenner, N., and Kang, H.: A regulatory role for phenol oxidase during decomposition in peatlands, *Soil Biology and Biochemistry*, 36, 1663–1667, <https://doi.org/10.1016/j.soilbio.2004.07.012>, 2004.
- Freitas, J. C. C., Passamani, E. C., Orlando, M. T. D., Emmerich, F. G., Garcia, F., Sampaio, L. C., and Bonagamba, T. J.: Effects of Ferromagnetic Inclusions on <sup>13</sup>C MAS NMR Spectra of Heat-Treated Peat Samples, *Energy & Fuels*, 16, 1068–1075, <https://doi.org/10.1021/ef010283w>, 2002.



- 1000 Gadel, F. and Bruchet, A.: Application of Pyrolysis-Gas Chromatography-Mass Spectrometry to the Characterization of Humic Substances Resulting from Decay of Aquatic Plants in Sediments and Waters, *Water Research*, 21, 1195–1206, [https://doi.org/10.1016/0043-1354\(87\)90171-0](https://doi.org/10.1016/0043-1354(87)90171-0), 1987.
- Gallego-Sala, A. V., Charman, D. J., Brewer, S., Page, S. E., Prentice, I. C., Friedlingstein, P., Moreton, S., Amesbury, M. J., Beilman, D. W., Björck, S., Blyakharchuk, T., Bochicchio, C., Booth, R. K., Bunbury, J., Camill, P., Carless, D., Chimner, R. A., Clifford, M., Cressey, E., Courtney-Mustaphi, C., De Vleeschouwer, F., de Jong, R., Fialkiewicz-Kozziel, B., Finkelstein, S. A., Garneau, M., Githumbi, E., Hribljan, J., Holmquist, J., Hughes, P. D. M., Jones, C., Jones, M. C., Karofeld, E., Klein, E. S., Kokfelt, U., Korhola, A., Lacourse, T., Le Roux, G., Lamentowicz, M., Large, D., Lavoie, M., Loisel, J., Mackay, H., MacDonald, G. M., Makila, M., Magnan, G., Marchant, R., Marcisz, K., Martínez Cortizas, A., Massa, C., Mathijssen, P., Mauquoy, D., Mighall, T., Mitchell, F. J. G., Moss, P., Nichols, J., Oksanen, P. O., Orme, L., Packalen, M. S., Robinson, S., Roland, T. P., Sanderson, N. K., Sannel, A. B. K., Silva-Sánchez, N., Steinberg, N., Swindles, G. T., Turner, T. E., Uglow, J., Väliranta, M., van Bellen, S., van der Linden, M., van Geel, B., Wang, G., Yu, Z., Zaragoza-Castells, J., and Zhao, Y.: Latitudinal limits to the predicted increase of the peatland carbon sink with warming, *Nature Climate Change*, 8, 907–913, <https://doi.org/10.1038/s41558-018-0271-1>, 2018.
- 1005 Galletti, G. C. and Reeves, J. B.: Pyrolysis/gas chromatography/ion-trap detection of polyphenols (vegetable tannins): Preliminary results, *Organic Mass Spectrometry*, 27, 226–230, <https://doi.org/10.1002/oms.1210270313>, 1992.
- Girkin, N. T., Lopes dos Santos, R. A., Vane, C. H., Ostle, N., Turner, B. L., and Sjögersten, S.: Peat Properties, Dominant Vegetation Type and Microbial Community Structure in a Tropical Peatland, *Wetlands*, 40, 1367–1377, <https://doi.org/10.1007/s13157-020-01287-4>, 2020.
- 1020 Girkin, N. T., Cooper, H. V., Ledger, M. J., O’Reilly, P., Thornton, S. A., Åkesson, C. M., Cole, L. E. S., Hapsari, K. A., Hawthorne, D., and Roucoux, K. H.: Tropical peatlands in the Anthropocene: The present and the future, *Anthropocene*, 40, <https://doi.org/10.1016/j.ancene.2022.100354>, 2022.
- Given, P. H., Spackman, W., Painter, P. C., Rhoads, C. A., and Ryan, N. J.: The fate of cellulose and lignin in peats: an exploratory study of the input to coalification, *Organic Geochemistry*, 6, 399–407, 1984.
- 1025 Gunina, A. and Kuzyakov, Y.: From energy to (soil organic) matter, *Global Change Biology*, 28, 2169–2182, <https://doi.org/10.1111/gcb.16071>, 2022.
- Gupta, N. S., Collinson, M. E., Briggs, D. E. G., Evershed, R. P., and Pancost, R. D.: Reinvestigation of the occurrence of cutan in plants: implications for the leaf fossil record, *Paleobiology*, 32, 432–449, <https://doi.org/10.1666/05038.1>, 2006.
- 1030 Gupta, N. S., Michels, R., Briggs, D. E. G., Collinson, M. E., Evershed, R. P., and Pancost, R. D.: Experimental evidence for the formation of geomacromolecules from plant leaf lipids, *Organic Geochemistry*, 38, 28–36, <https://doi.org/10.1016/j.orggeochem.2006.09.014>, 2007a.
- Gupta, N. S., Briggs, D. E. G., Collinson, M. E., Evershed, R. P., Michels, R., Jack, K. S., and Pancost, R. D.: Evidence for the in situ polymerisation of labile aliphatic organic compounds during the preservation of fossil leaves: Implications for organic matter preservation, *Organic Geochemistry*, 38, 499–522, <https://doi.org/10.1016/j.orggeochem.2006.06.011>, 2007b.
- 1035 Hedges, J. I. and Mann, D. C.: The characterization of plant tissues by their lignin oxidation products, *Geochimica et Cosmochimica Acta*, 43, 1803–1807, [https://doi.org/10.1016/0016-7037\(79\)90028-0](https://doi.org/10.1016/0016-7037(79)90028-0), 1979.
- Hedges, J. I., Cowie, G. L., Ertel, J. R., Barbour, R. J., and Hatcher, P. G.: Degradation of carbohydrates and lignins in buried woods, *Geochimica et Cosmochimica Acta*, 49, 701–711, [https://doi.org/10.1016/0016-7037\(85\)90165-6](https://doi.org/10.1016/0016-7037(85)90165-6), 1985.



- 1040 Hodgkins, S. B., Richardson, C. J., Dommoin, R., Wang, H., Glaser, P. H., Verbeke, B., Winkler, B. R., Cobb, A. R., Rich, V. I., Missilmani, M., Flanagan, N., Ho, M., Hoyt, A. M., Harvey, C. F., Vining, S. R., Hough, M. A., Moore, T. R., Richard, P. J. H., De La Cruz, F. B., Toufaily, J., Hamdan, R., Cooper, W. T., and Chanton, J. P.: Tropical peatland carbon storage linked to global latitudinal trends in peat recalcitrance, *Nature Communications*, 9, 3640, <https://doi.org/10.1038/s41467-018-06050-2>, 2018.
- Hornibrook, E. R. C. and Bowes, H. L.: Trophic status impacts both the magnitude and stable carbon isotope composition of methane flux from peatlands, *Geophysical Research Letters*, 34, <https://doi.org/10.1029/2007gl031231>, 2007.
- 1045 Hou, J., Wang, Y., Zhu, P., Yang, N., Liang, L., Yu, T., Niu, M., Konhauser, K., Woodcroft, B. J., and Wang, F.: Taxonomic and carbon metabolic diversification of Bathyarchaeia during its coevolution history with early Earth surface environment, *Science Advances*, 9, <https://doi.org/10.1126/sciadv.adf5069>, 2023.
- Hoyos-Santillan, J., Lomax, B. H., Large, D., Turner, B. L., Boom, A., Lopez, O. R., and Sjögersten, S.: Getting to the root of the problem: litter decomposition and peat formation in lowland Neotropical peatlands, *Biogeochemistry*, 126, 115–129, <https://doi.org/10.1007/s10533-015-0147-7>, 2015.
- 1050 Hoyos-Santillan, J., Lomax, B. H., Large, D., Turner, B. L., Boom, A., Lopez, O. R., and Sjögersten, S.: Quality not quantity: Organic matter composition controls of CO<sub>2</sub> and CH<sub>4</sub> fluxes in neotropical peat profiles, *Soil Biology and Biochemistry*, 103, 86–96, <https://doi.org/10.1016/j.soilbio.2016.08.017>, 2016.
- Hoyos-Santillan, J., Lomax, B. H., Turner, B. L., Sjögersten, S., and Austin, A.: Nutrient limitation or home field advantage: Does microbial community adaptation overcome nutrient limitation of litter decomposition in a tropical peatland?, *Journal of Ecology*, 106, 1558–1569, <https://doi.org/10.1111/1365-2745.12923>, 2017.
- 1055 Hughes, P. D. M. and Dumayne-Peaty, L.: Testing theories of mire development using multiple successions at Crymlyn Bog, West Glamorgan, South Wales, UK, *Journal of Ecology*, 90, 456–471, <https://doi.org/10.1046/j.1365-2745.2002.00677.x>, 2002.
- 1060 Inglett, K. S., Inglett, P. W., Reddy, K. R., and Osborne, T. Z.: Temperature in wetland sensitivity of greenhouse soils of different vegetation, *Biogeochemistry*, 108, 77–90, <https://doi.org/10.1007/S10533-01>, 2012.
- James, G., Witten, D., Hastie, T., and Tibshirani, R.: *An Introduction to Statistical Learning with Applications in R*, Springer Texts in Statistics, 2013.
- 1065 Janusz, G., Pawlik, A., Sulej, J., Swiderska-Burek, U., Jarosz-Wilkolazka, A., and Paszczynski, A.: Lignin degradation: microorganisms, enzymes involved, genomes analysis and evolution, *FEMS Microbiology Reviews*, 41, 941–962, <https://doi.org/10.1093/femsre/fux049>, 2017.
- Janusz, G., Pawlik, A., Swiderska-Burek, U., Polak, J., Sulej, J., Jarosz-Wilkolazka, A., and Paszczynski, A.: Laccase Properties, Physiological Functions, and Evolution, *Int. J. Mol. Sci.*, 21, <https://doi.org/10.3390/ijms21030966>, 2020.
- 1070 Juottonen, H., Eiler, A., Biasi, C., Tuittila, E. S., Yrjala, K., and Fritze, H.: Distinct Anaerobic Bacterial Consumers of Cellobiose-Derived Carbon in Boreal Fens with Different CO<sub>2</sub>/CH<sub>4</sub> Production Ratios, *Applied Environmental Microbiology*, 83, <https://doi.org/10.1128/AEM.02533-16>, 2017.
- Kaal, J., Cortizas, A. M., and Biester, H.: Downstream changes in molecular composition of DOM along a headwater stream in the Harz mountains (Central Germany) as determined by FTIR, Pyrolysis-GC-MS and THM-GC-MS, *Journal of Analytical and Applied Pyrolysis*, 126, 50–61, <https://doi.org/10.1016/j.jaap.2017.06.025>, 2017.



- 1075 Kaal, J., Baldock, J. A., Buurman, P., Nierop, K. G. J., Pontevedra-Pombal, X., and Martínez-Cortizas, A.: Evaluating pyrolysis–GC/MS and <sup>13</sup>C CPMAS NMR in conjunction with a molecular mixing model of the Penido Vello peat deposit, NW Spain, *Organic Geochemistry*, 38, 1097–1111, <https://doi.org/10.1016/j.orggeochem.2007.02.008>, 2007.
- Kayendeke, E. J., Kansime, F., French, H. K., and Bamutaze, Y.: Spatial and temporal variation of papyrus root mat thickness and water storage in a tropical wetland system, *Science of the Total Environment*, 642, 925–936, <https://doi.org/10.1016/j.scitotenv.2018.06.087>, 2018.
- 1080
- Kim, K., Aernouts, B., Emsens, W.-J., Schellekens, J., van Diggelen, R., Aggenbach, C., Verbruggen, E., Jansen, B., Briones, M. J. I., and Vancampenhout, K.: Mid-infrared spectroscopy as a tool to monitor molecular changes in fens upon restoration, *Organic Geochemistry*, 214, <https://doi.org/10.1016/j.orggeochem.2026.105154>, 2026.
- Klein, J. K.: A molecular approach to the assessment of peat organic matter – investigating ecosystem-driven differences in chemical composition, *Philosophisch-Naturwissenschaftlichen Fakultät, Universität Basel, Basel, Switzerland*, 2022.
- 1085
- Klein, K., Gross-Schmölders, M., De la Rosa, J. M., Alewell, C., and Leifeld, J.: Investigating the influence of instrumental parameters and chemical composition on pyrolysis efficiency of peat, *Communications in Soil Science and Plant Analysis*, 51, 1572–1581, <https://doi.org/10.1080/00103624.2020.1784916>, 2020.
- Klein, K., Schellekens, J., Groß-Schmölders, M., von Sengbusch, P., Alewell, C., and Leifeld, J.: Characterizing ecosystem-driven chemical composition differences in natural and drained Finnish bogs using pyrolysis-GC/MS, *Organic Geochemistry*, 165, <https://doi.org/10.1016/j.orggeochem.2021.104351>, 2022.
- 1090
- Könönen, M., Jauhiainen, J., Laiho, R., Spetz, P., Kusin, K., Limin, S., and Vasander, H.: Land use increases the recalcitrance of tropical peat, *Wetlands Ecology and Management*, 24, 717–731, <https://doi.org/10.1007/s11273-016-9498-7>, 2016.
- 1095
- Lehtonen, K. and Ketola, M.: Solvent-extractable lipids of Sphagnum, Carex, Bryales and Carex-Bryales peats: content and compositional features vs peat humification, *Organic Geochemistry*, 20, 363–380, [https://doi.org/10.1016/0146-6380\(93\)90126-y](https://doi.org/10.1016/0146-6380(93)90126-y), 1993.
- Leifeld, J. and Menichetti, L.: The underappreciated potential of peatlands in global climate change mitigation strategies, *Nature Communications*, 9, 1071, <https://doi.org/10.1038/s41467-018-03406-6>, 2018.
- 1100
- Leifeld, J., Wüst-Galley, C., and Page, S.: Intact and managed peatland soils as a source and sink of GHGs from 1850 to 2100, *Nature Climate Change*, 9, 945–947, <https://doi.org/10.1038/s41558-019-0615-5>, 2019.
- Lichtfouse, É., Dou, S., Girardin, C., Grably, M., Balesdent, J., Behar, F., and Vandenbroucke, M.: Unexpected <sup>13</sup>C-enrichment of organic components from wheat crop soils: evidence for the in situ origin of soil organic matter, *Organic Geochemistry*, 23, 865–868, [https://doi.org/10.1016/0146-6380\(95\)80009-g](https://doi.org/10.1016/0146-6380(95)80009-g), 1995.
- 1105
- Liu, T., Li, L., Xue, K., Wang, X., Li, H., Wang, Y., and Dong, X.: Methane production from lignin in anoxic peatland, *Nature Geoscience*, 18, 877–884, <https://doi.org/10.1038/s41561-025-01758-5>, 2025.
- Loisel, J., Gallego-Sala, A. V., Amesbury, M. J., Magnan, G., Anshari, G., Beilman, D. W., Benavides, J. C., Blewett, J., Camill, P., Charman, D. J., Chawchai, S., Hedgpeth, A., Kleinen, T., Korhola, A., Large, D., Mansilla, C. A., Müller, J., van Bellen, S., West, J. B., Yu, Z., Bubier, J. L., Garneau, M., Moore, T., Sannel, A. B. K., Page, S., Väliranta, M., Bechtold, M., Brovkin, V., Cole, L. E. S., Chanton, J. P., Christensen, T. R., Davies, M. A., De Vleeschouwer, F., Finkelstein, S. A., Frolking, S., Galka, M., Gandois, L., Girkin, N., Harris, L. I., Heinemeyer, A., Hoyt, A. M., Jones, M. C., Joos, F., Juutinen, S., Kaiser, K., Lacourse, T., Lamentowicz, M., Larmola, T., Leifeld, J., Lohila, A., Milner, A. M., Minkinen, K., Moss, P.,
- 1110



- 1115 Naafs, B. D. A., Nichols, J., O'Donnell, J., Payne, R., Philben, M., Piilo, S., Quillet, A., Ratnayake, A. S., Roland, T. P., Sjögersten, S., Sonntag, O., Swindles, G. T., Swinnen, W., Talbot, J., Treat, C., Valach, A. C., and Wu, J.: Expert assessment of future vulnerability of the global peatland carbon sink, *Nature Climate Change*, 11, 70–77, <https://doi.org/10.1038/s41558-020-00944-0>, 2020.
- Lorenz, K., Lal, R., Preston, C. M., and Nierop, K. G. J.: Strengthening the soil organic carbon pool by increasing contributions from recalcitrant aliphatic bio(macro)molecules, *Geoderma*, 142, 1–10, <https://doi.org/10.1016/j.geoderma.2007.07.013>, 2007.
- 1120 McClymont, E. L., Bingham, E. M., Nott, C. J., Chambers, F. M., Pancost, R. D., and Evershed, R. P.: Pyrolysis GC–MS as a rapid screening tool for determination of peat-forming plant composition in cores from ombrotrophic peat, *Organic Geochemistry*, 42, 1420–1435, <https://doi.org/10.1016/j.orggeochem.2011.07.004>, 2011.
- McGivern, B. B., Tfaily, M. M., Borton, M. A., Kosina, S. M., Daly, R. A., Nicora, C. D., Purvine, S. O., Wong, A. R., Lipton, M. S., Hoyt, D. W., Northen, T. R., Hagerman, A. E., and Wrighton, K. C.: Decrypting bacterial polyphenol metabolism in an anoxic wetland soil, *Nature Communications*, 12, 2466, <https://doi.org/10.1038/s41467-021-22765-1>, 2021.
- Melillo, J. M., Aber, J. D., Linkins, A. E., Ricca, A., Fry, B., and Nadelhoffer, K. J.: Carbon and nitrogen dynamics along the decay continuum: Plant litter to soil organic matter, *Plant and Soil*, 115, 189–198, <https://doi.org/10.1007/BF02202587>, 1989.
- 1130 Michel, S. E., Lan, X., Miller, J., Tans, P., Clark, J. R., Schaefer, H., Sperlich, P., Brailsford, G., Morimoto, S., Moossen, H., and Li, J.: Rapid shift in methane carbon isotopes suggests microbial emissions drove record high atmospheric methane growth in 2020–2022, *Proc. Natl. Acad. Sci. U. S. A.*, 121, e2411212121, <https://doi.org/10.1073/pnas.2411212121>, 2024.
- Moers, M. E. C., Baas, M., Boon, J. J., and De Leeuw, J. W.: Molecular characterization of total organic matter and carbohydrates in peat samples from a cypress swamp by pyrolysis-mass spectrometry and wet-chemical methods, *Biogeochemistry*, 11, 251–277, <https://doi.org/10.1007/BF00004499>, 1990.
- 1135 Moody, C. S., Worrall, F., Clay, G. D., Burt, T. P., Apperley, D. C., and Rose, R.: A Molecular Budget for a Peatland Based Upon <sup>13</sup>C Solid-State Nuclear Magnetic Resonance, *Journal of Geophysical Research: Biogeosciences*, 123, 547–560, <https://doi.org/10.1002/2017jg004312>, 2018.
- Nichols, J. E. and Peteet, D. M.: Rapid expansion of northern peatlands and doubled estimate of carbon storage, *Nature Geoscience*, 12, 917–921, <https://doi.org/10.1038/s41561-019-0454-z>, 2019.
- 1140 Nierop, K. G. J.: Origin of aliphatic compounds in a forest soil, *Organic Geochemistry*, 29, 1009–1016, [https://doi.org/10.1016/S0146-6380\(98\)00165-X](https://doi.org/10.1016/S0146-6380(98)00165-X), 1998.
- Nierop, K. G. J. and van Bergen, P. F.: Clay and ammonium catalyzed reactions of alkanols, alkanolic acids and esters under flash pyrolytic conditions, *Journal of Analytical and Applied Pyrolysis*, 63, 197–208, [https://doi.org/10.1016/S0165-2370\(01\)00154-1](https://doi.org/10.1016/S0165-2370(01)00154-1), 2002.
- 1145 Normand, A. E., Turner, B. L., Lamit, L. J., Smith, A. N., Baiser, B., Clark, M. W., Hazlett, C., Kane, E. S., Lilleskov, E., Long, J. R., Grover, S. P., and Reddy, K. R.: Organic Matter Chemistry Drives Carbon Dioxide Production of Peatlands, *Geophysical Research Letters*, 48, <https://doi.org/10.1029/2021gl093392>, 2021.



- 1150 Nott, C. J., Xie, S., Avsejs, L. A., Maddy, D., Chambers, F. M., and Evershed, R. P.: n-Alkane distributions in ombrotrophic mires as indicators of vegetation change related to climatic variation, *Organic geochemistry*, 31, 231–235, [https://doi.org/10.1016/S0146-6380\(99\)00153-9](https://doi.org/10.1016/S0146-6380(99)00153-9), 2000.
- Ortiz, O. O., Ibáñez, A., Trujillo-Trujillo, E., and Croat, T. B.: The emergent macrophyte *Montrichardia linifera* (Arruda) Schott (Alismatales: Araceae), a rekindled old friend from the Pacific Slope of lower Central America and western Colombia, *Nordic Journal of Botany*, 38, <https://doi.org/10.1111/njb.02832>, 2020.
- 1155 Page, S., Mishra, S., Agus, F., Anshari, G., Dargie, G., Evers, S., Jauhainen, J., Jaya, A., Jovani-Sancho, A. J., Laurén, A., Sjögersten, S., Suspense, I. A., Wijedasa, L. S., and Evans, C. D.: Anthropogenic impacts on lowland tropical peatland biogeochemistry, *Nature Reviews Earth & Environment*, 3, 426–443, <https://doi.org/10.1038/s43017-022-00289-6>, 2022.
- Page, S. E. and Baird, A. J.: Peatlands and Global Change: Response and Resilience, *Annual Review of Environment and Resources*, 41, 35–57, <https://doi.org/10.1146/annurev-environ-110615-085520>, 2016.
- 1160 Pavia, M.: Microbial Functions and Interactions in Carbon Cycling of Amazon Peatlands, School of Life Sciences, Arizona State University, Tempe, United States, 2024.
- Pavia, M. J., Garber, A. I., Avalle, S., Macedo-Tafur, F., Tello-Espinoza, R., and Cadillo-Quiroz, H.: Functional insights of novel Bathyarchaeia reveal metabolic versatility in their role in peatlands of the Peruvian Amazon, *Microbiology Spectrum*, 12, <https://doi.org/10.1128/spectrum.00387-24>, 2024.
- 1165 Peng, S., Lin, X., Thompson, R. L., Xi, Y., Liu, G., Hauglustaine, D., Lan, X., Poulter, B., Ramonet, M., Saunio, M., Yin, Y., Zhang, Z., Zheng, B., and Ciais, P.: Wetland emission and atmospheric sink changes explain methane growth in 2020, *Nature*, 612, 477–482, <https://doi.org/10.1038/s41586-022-05447-w>, 2022.
- Phillips, S., Rouse, G. E., and Bustin, R. M.: Vegetation zones and diagnostic pollen profiles of a coastal peat swamp, Bocas del Toro, Panama, *Palaeogeography, Palaeoclimatology, Palaeoecology*, 128, 301–338, [https://doi.org/10.1016/S0031-0182\(97\)81129-7](https://doi.org/10.1016/S0031-0182(97)81129-7), 1997.
- 1170 R Core Team: R: A Language and Environment for Statistical Computing, 2025.
- Reig, F. B., Gimeno Adelantado, J. V., and Moya Moreno, M. C. M.: FTIR quantitative analysis of calcium carbonate (calcite) and silica (quartz) mixtures using the constant ratio method. Application to geological samples, *Talanta*, 58, 811–821, [https://doi.org/10.1016/S0039-9140\(02\)00372-7](https://doi.org/10.1016/S0039-9140(02)00372-7), 2002.
- 1175 Ring-Hrubesh, F., Vreeken, M., Eberle, A., Welch, B., Sinnadurai, P., Johnes, P., Griffiths, R., Gallego-Sala, A., Pancost, R., and Bryce, C.: Legacy of peatland erosion shapes microbial communities during recovery, *eartharxiv*, <https://doi.org/10.31223/X5RT8J>, 2025.
- Rosset, T., Binet, S., Rigal, F., and Gandois, L.: Peatland Dissolved Organic Carbon Export to Surface Waters: Global Significance and Effects of Anthropogenic Disturbance, *Geophysical Research Letters*, 49, <https://doi.org/10.1029/2021gl096616>, 2022.
- 1180 Ryan, N. J., Given, P. H., Boon, J. J., and de Leeuw, J. W.: Study of the fate of plant polymers in peats by Curie-point pyrolysis, *International Journal of Coal Geology*, 8, 85–98, [https://doi.org/10.1016/0166-5162\(87\)90024-3](https://doi.org/10.1016/0166-5162(87)90024-3), 1987.
- Saiz-Jimenez, C. and de Leeuw, J. W.: Lignin pyrolysis products: Their structures and their significance as biomarkers, *Organic Geochemistry*, 10, 869–876, [https://doi.org/10.1016/S0146-6380\(86\)80024-9](https://doi.org/10.1016/S0146-6380(86)80024-9), 1986.



- 1185 Schellekens, J.: The use of molecular chemistry (pyrolysis-GC/MS) in the environmental interpretation of peat, Department of Soil Quality, Wageningen University, Wageningen, the Netherlands, 2013.
- Schellekens, J. and Buurman, P.: n-Alkane distributions as palaeoclimatic proxies in ombrotrophic peat: The role of decomposition and dominant vegetation, *Geoderma*, 164, 112–121, <https://doi.org/10.1016/j.geoderma.2011.05.012>, 2011.
- 1190 Schellekens, J., Buurman, P., and Kuyper, T. W.: Source and transformations of lignin in *Carex*-dominated peat, *Soil Biology and Biochemistry*, 53, 32–42, <https://doi.org/10.1016/j.soilbio.2012.04.030>, 2012.
- Schellekens, J., Buurman, P., and Pontevedra-Pombal, X.: Selecting parameters for the environmental interpretation of peat molecular chemistry – A pyrolysis-GC/MS study, *Organic Geochemistry*, 40, 678–691, <https://doi.org/10.1016/j.orggeochem.2009.03.006>, 2009.
- 1195 Schellekens, J., Buurman, P., Kuyper, T. W., Abbott, G. D., Pontevedra-Pombal, X., and Martínez-Cortizas, A.: Influence of source vegetation and redox conditions on lignin-based decomposition proxies in graminoid-dominated ombrotrophic peat (Penido Vello, NW Spain), *Geoderma*, 237–238, 270–282, <https://doi.org/10.1016/j.geoderma.2014.09.012>, 2015.
- Scheller, H. V. and Ulvskov, P.: Hemicelluloses, *Annual Review of Plant Biology*, 61, 263–289, <https://doi.org/10.1146/annurev-arplant-042809-112315>, 2010.
- 1200 Shafizadeh, F. and Fu, Y. L.: Pyrolysis of cellulose, *Carbohydrate Research*, 29, 113–122, [https://doi.org/10.1016/S0008-6215\(00\)82074-1](https://doi.org/10.1016/S0008-6215(00)82074-1), 1973.
- Sihi, D., Inglett, P. W., and Inglett, K. S.: Carbon quality and nutrient status drive the temperature sensitivity of organic matter decomposition in subtropical peat soils, *Biogeochemistry*, 131, 103–119, <https://doi.org/10.1007/s10533-016-0267-8>, 2016.
- 1205 Sjögersten, S., Cheesman, A. W., Lopez, O., and Turner, B. L.: Biogeochemical processes along a nutrient gradient in a tropical ombrotrophic peatland, *Biogeochemistry*, 104, 147–163, <https://doi.org/10.1007/s10533-010-9493-7>, 2011.
- Sjögersten, S., Aplin, P., Gauci, V., Peacock, M., Siegenthaler, A., and Turner, B. L.: Temperature response of ex-situ greenhouse gas emissions from tropical peatlands: Interactions between forest type and peat moisture conditions, *Geoderma*, 324, 47–55, <https://doi.org/10.1016/j.geoderma.2018.02.029>, 2018.
- 1210 Stankiewicz, A. B., van Bergen, P. F., Duncan, I. J., Carter, J. F., Briggs, D. E. G., and Evershed, R. P.: Recognition of Chitin and Proteins in Invertebrate Cuticles Using Analytical Pyrolysis/Gas Chromatography and Pyrolysis/Gas Chromatography/Mass Spectrometry, *Rapid Communications in Mass Spectrometry*, 10, 1747–1757, [https://doi.org/10.1002/\(SICI\)1097-0231\(199611\)10:14<1747::AID-RCM713>3.0.CO;2-H](https://doi.org/10.1002/(SICI)1097-0231(199611)10:14<1747::AID-RCM713>3.0.CO;2-H), 1996.
- Stankiewicz, B. A., Briggs, D. E. G., Michels, R., Collinson, M. E., Flannery, M. B., and Evershed, R. P.: Alternative origin of aliphatic polymer in kerogen, *Geology*, 28, 559–562, [https://doi.org/10.1130/0091-7613\(2000\)28](https://doi.org/10.1130/0091-7613(2000)28), 2000.
- 1215 Swindles, G. T., Whitney, B. S., Gałka, M., Mullan, D. J., Low, R., Gallego-Sala, A., Lopez, R. O., Kilbride, E., Graham, C., and Baird, A. J.: Ecohydrological Response of a Tropical Peatland to Rainfall Changes Driven by Intertropical Convergence Zone Variability, *Journal of Biogeography*, 52, 621–628, <https://doi.org/10.1111/jbi.15051>, 2024.
- Thormann, M. N.: Diversity and function of fungi in peatlands: a carbon cycling perspective, *Canadian journal of soil science*, 86, 281–293, <https://doi.org/10.4141/S05-082>, 2006.



- 1220 Too, C. C., Keller, A., Sickel, W., Lee, S. M., and Yule, C. M.: Microbial Community Structure in a Malaysian Tropical Peat Swamp Forest: The Influence of Tree Species and Depth, *Frontiers in Microbiology*, 9, 2859, <https://doi.org/10.3389/fmicb.2018.02859>, 2018.
- Troxler, T. G.: Patterns of phosphorus, nitrogen and  $\delta^{15}\text{N}$  along a peat development gradient in a coastal mire, Panama, *Journal of Tropical Ecology*, 23, 683–691, <https://doi.org/10.1017/s0266467407004464>, 2007.
- 1225 Uhelski, D. M., Kane, E. S., and Chimner, R. A.: Plant functional types drive Peat Quality differences, *Wetlands*, 42, <https://doi.org/10.1007/s13157-022-01572-4>, 2022.
- Upton, A., Vane, C. H., Girkin, N., Turner, B. L., and Sjögersten, S.: Does litter input determine carbon storage and peat organic chemistry in tropical peatlands?, *Geoderma*, 326, 76–87, <https://doi.org/10.1016/j.geoderma.2018.03.030>, 2018.
- 1230 Urbanova, Z. and Hajek, T.: Revisiting the concept of 'enzymic latch' on carbon in peatlands, *Science of the Total Environment*, 779, 146384, <https://doi.org/10.1016/j.scitotenv.2021.146384>, 2021.
- van der Heijden, E. and Boon, J. J.: A combined pyrolysis mass spectrometric and light microscopic study of peatified Calluna wood isolated from raised bog peat deposits, *Organic Geochemistry*, 22, 903–919, [https://doi.org/10.1016/0146-6380\(94\)90028-0](https://doi.org/10.1016/0146-6380(94)90028-0), 1994.
- 1235 Van der Heijden, E., Boon, J. J., Rasmussen, S., and Rudolph, H.: Sphagnum acid and its decarboxylation product isopropenylphenol as biomarkers for fossilised Sphagnum in peats, *Ancient Biomolecules*, 1, 93–107, 1997.
- Verbeke, B. A., Lamit, L. J., Lilleskov, E. A., Hodgkins, S. B., Basiliko, N., Kane, E. S., Andersen, R., Artz, R. R. E., Benavides, J. C., Benschoter, B. W., Borken, W., Bragazza, L., Brandt, S. M., Bräuer, S. L., Carson, M. A., Charman, D., Chen, X., Clarkson, B. R., Cobb, A. R., Convey, P., Pasquel, J. d. Á., Enriquez, A. S., Griffiths, H., Grover, S. P., Harvey, C. F., Harris, L. I., Hazard, C., Hodgson, D., Hoyt, A. M., Hribljan, J., Jauhiainen, J., Juutinen, S., Knorr, K. H., Kolka, R. K., 1240 Kõnönen, M., Larmola, T., McCalley, C. K., McLaughlin, J., Moore, T. R., Mykityczuk, N., Normand, A. E., Rich, V., Roulet, N., Royles, J., Rutherford, J., Smith, D. S., Svenning, M. M., Tedersoo, L., Thu, P. Q., Trettin, C. C., Tuittila, E. S., Urbanová, Z., Varner, R. K., Wang, M., Wang, Z., Warren, M., Wiedermann, M. M., Williams, S., Yavitt, J. B., Yu, Z. G., Yu, Z., and Chanton, J. P.: Latitude, Elevation, and Mean Annual Temperature Predict Peat Organic Matter Chemistry at a Global Scale, *Global Biogeochemical Cycles*, 36, <https://doi.org/10.1029/2021gb007057>, 2022.
- 1245 Wang, H., Waldon, M. G., Meselhe, E. A., Arceneaux, J. C., Chen, C., and Harwell, M. C.: Surface water sulfate dynamics in the northern Florida Everglades, *J. Environ. Qual.*, 38, 734–741, <https://doi.org/10.2134/jeq2007.0455>, 2009.
- Wang, H., Tian, J., Chen, H., Ho, M., Vilgalys, R., Bu, Z.-J., Liu, X., and Richardson, C. J.: Vegetation and microbes interact to preserve carbon in many wooded peatlands, *Communications Earth & Environment*, 2, <https://doi.org/10.1038/s43247-021-00136-4>, 2021.
- 1250 Weng, J. K. and Chapple, C.: The origin and evolution of lignin biosynthesis, *New Phytologist*, 187, 273–285, <https://doi.org/10.1111/j.1469-8137.2010.03327.x>, 2010.
- West, S.: Geochemical and palynological signals for palaeoenvironmental change in south west England, Department of Geographical Sciences, University of Plymouth, Plymouth, United Kingdom, 10.24382/3569, 1997.
- 1255 Winton, R. S., Benavides, J. C., Mendoza, E., Uhde, A., Hastie, A., Honorio Coronado, E. N., Hernandez Ortega, A. G., Paukku, S., Mullins, B., del Aguila Pasquel, J., Aymard-Corredor, G. A., Baker, T. R., Draper, F. C., Flores Llampazo, G., Herrera, R., Phillips, O. L., Reyna Huaymacari, J. M., ter Steege, H., Stropp, J., Lawson, I. T., Gallego-Sala, A. V., Boom,



- A., Wehrli, B., and Hoyt, A. M.: Widespread carbon-dense peatlands in the Colombian lowlands, *Environmental Research Letters*, 20, <https://doi.org/10.1088/1748-9326/adb03>, 2025.
- 1260 Wright, A. L., Reddy, K. R., and Newman, S.: Biogeochemical response of the Everglades landscape to eutrophication, *Global Journal of Environmental Science and Management*, 2, 102–109, 2008.
- Wright, E. L., Black, C. R., Turner, B. L., and Sjoogersten, S.: Environmental controls of temporal and spatial variability in CO<sub>2</sub> and CH<sub>4</sub> fluxes in a neotropical peatland, *Global Change Biology*, 19, 3775–3789, <https://doi.org/10.1111/gcb.12330>, 2013.
- 1265 Wright, E. L., Black, C. R., Cheesman, A. W., Drage, T., Large, D., Turner, B. L., and Sjoogersten, S.: Contribution of subsurface peat to CO<sub>2</sub> and CH<sub>4</sub> fluxes in a neotropical peatland, *Global Change Biology*, 17, 2867–2881, <https://doi.org/10.1111/j.1365-2486.2011.02448.x>, 2011.
- Wright, W. and Comas, X.: Estimating methane gas production in peat soils of the Florida Everglades using hydrogeophysical methods, *Journal of Geophysical Research: Biogeosciences*, 121, 1190–1202, <https://doi.org/10.1002/2015jg003246>, 2016.
- 1270 Xiong, Y., Kort, E. A., Bloom, A. A., Gerlein-Safdi, C., Pu, T., and Bilir, E.: Limited evidence that tropical inundation and precipitation powered the 2020-2022 methane surge, *Communications Earth & Environment*, 6, 450, <https://doi.org/10.1038/s43247-025-02438-3>, 2025.
- Yarwood, S. A.: The role of wetland microorganisms in plant-litter decomposition and soil organic matter formation: a critical review, *FEMS Microbiology Ecology*, 94, <https://doi.org/10.1093/femsec/fiy175>, 2018.
- 1275 Young, D. M., Baird, A. J., Gallego-Sala, A. V., and Loisel, J.: A cautionary tale about using the apparent carbon accumulation rate (aCAR) obtained from peat cores, *Scientific Reports*, 11, 9547, <https://doi.org/10.1038/s41598-021-88766-8>, 2021.
- Yu, T., Hu, H., Zeng, X., Wang, Y., Pan, D., and Wang, F.: Cultivation of widespread Bathyarchaeia reveals a novel methyltransferase system utilizing lignin-derived aromatics, *bioRxiv*, <https://doi.org/10.1101/2022.10.23.513425>, 2022.
- 1280 Yu, T., Wu, W., Liang, W., Lever, M. A., Hinrichs, K. U., and Wang, F.: Growth of sedimentary Bathyarchaeota on lignin as an energy source, *Proc. Natl. Acad. Sci. U. S. A.*, 115, 6022–6027, <https://doi.org/10.1073/pnas.1718854115>, 2018.
- Yu, Z., Loisel, J., Brosseau, D. P., Beilman, D. W., and Hunt, S. J.: Global peatland dynamics since the Last Glacial Maximum, *Geophysical Research Letters*, 37, <https://doi.org/10.1029/2010gl043584>, 2010.